Detrital gold as a deposit-specific indicator mineral by LA-ICP-MS analysis

D.A. Banks, R.J. Chapman, C. Spence-Jones.
Ores and Mineralization Group School of Earth and Environment, the University, Leeds, UK

Geoscience BC Report 2018-21

Abstract

Gold derived from alkalic porphyry systems in BC has previously been shown to exhibit a generic Hg-Pd signature revealed in both alloy composition and the suite of minerals present as inclusions within gold particles. Development of an indicator mineral methodology based on this result has been hindered by the number of gold detrital gold grains required to confidently establish a signature, and the associated implications for the design of field exploration campaigns.

Trace element analysis of detrital gold grains has been undertaken using Laser-Inductively Coupled Plasma Mass Spectrometry (LA-ICP-MS) in an attempt to identify more elemental discriminants than has been possible by analysis using electron microprobe (EMP), and consequently reduce the sample size necessary for accurate characterization. Two LA-ICP-MS instruments have been used which collect data in different ways. The quadrupole system has been applied to all grains studied. The mass spectrometer sequentially scans the plasma stream to generate an analysis of material liberated by continual ablation. In contrast, the Time of Flight (ToF) instrument makes a single ablation, but measures all elements simultaneously. This approach has been used with only a few samples, but has generated new understanding of the heterogeneity of natural gold.

Consideration of the large element suite generated by LA-ICP-MS confirmed the elemental associations previously identified, and has facilitated characterization of gold populations in terms of the binary Au-Ag alloy and occurrence of minor alloying metals. Orogenic gold grains generate analyses which lie along a Au-Ag binary mixing line, but many gold grains from alkalic porphyry systems show clear deviation from this trend. Natural gold has been shown to be highly heterogeneous at the trace element level. Comparison of results from a LA quadrupole and a ToF system revealed that only a small number of elements are homogenously distributed in Au alloy. Most are present either as local concentrations or as inclusions of minerals too small to observe by SEM. This heterogeneity has profound implications for the interpretation of LA-ICP-MS data of natural gold generated by quadrupole systems, as the analyses obtained may be dependent upon the site of ablation within any particular gold grain.

The application of LA-ICP-MS to detrital gold grain characterization during exploration does not currently offer an advantage to the established workflow of microchemical characterization which measures alloy compositions using EMP and identifies the associated inclusions using SEM. Both microchemical characterization and LA-ICP-MS approaches currently require approximately equivalent numbers of detrital gold particles to generate useful information. However, the results of this study have raised the possibility that extreme partitioning of trace elements to mineral inclusions within the gold could form the basis of a methodology by which individual gold grains could be confidently ascribed to a specific source style.

Introduction

Exploration for porphyry mineralization is increasingly focussed on techniques which can identify mineralization concealed by Quaternary cover. Studies of the trace element mineralogy of minerals formed in porphyry systems (e.g. Bouzari et al., 2010, 2016; Celis et al., 2014; Pisiak et al., 2014) have identified mineralogical markers indicative of the environment of formation within an evolving magmatic hydrothermal system. The overall aim of these studies has been to permit informed interrogation of heavy mineral concentrates (HMC) collected during exploration campaigns.

Native gold grains derived from such mineralization may also be present in panned concentrates. However the simple presence of gold grains is not necessarily indicative of derivation from the exploration target. For example, Kelley (2011) reported that the nature of gold dispersion trains in glacial sediments in the environs of the Pebble porphyry, Alaska, may have been influenced by the influx of gold from different sources. The dispersion of particulate gold from the Mt. Polley porphyry deposit through glacial transport was investigated by Plouffe et al. (2013), who noted that the presence of a large auriferous paleoplacer deposit lying stratigraphically below till near the deposit could have resulted in gold grains being recycled into the more recent sediments. The information flowing from the identification and character of particulate gold in HMC would be far greater if it were possible to establish their genetic origins.

Studies of gold grain chemistry have been undertaken by several workers since the advent of the electron microprobe, which facilitates rapid determination of the major alloying elements (Ag, Cu, Hg, Pd) within native gold particles. Antweiler and Campbell (1979), identified systematic spatial variation in both Ag and Cu contents of native gold in the environs of Circle City, and speculated that gold composition was a consequence of the temperature at which the source mineralization was emplaced. Subsequent studies in important placer districts (e.g. the Cariboo, McTaggart and Knight, 1993, and the Klondike, Knight et al. 1999) also identified variation in the alloy compositions of populations of gold grains collected from different localities. Knight et al. (1999) applied these data to speculate that some in situ sources of Klondike placer gold remained to be discovered.

In the late 1980's the British Geological Survey developed a refined approach to gold grain characterization which involved systematic screening of grain sections to identify inclusions of other minerals preserved within the gold grains. They successfully correlated inclusion suites with variation

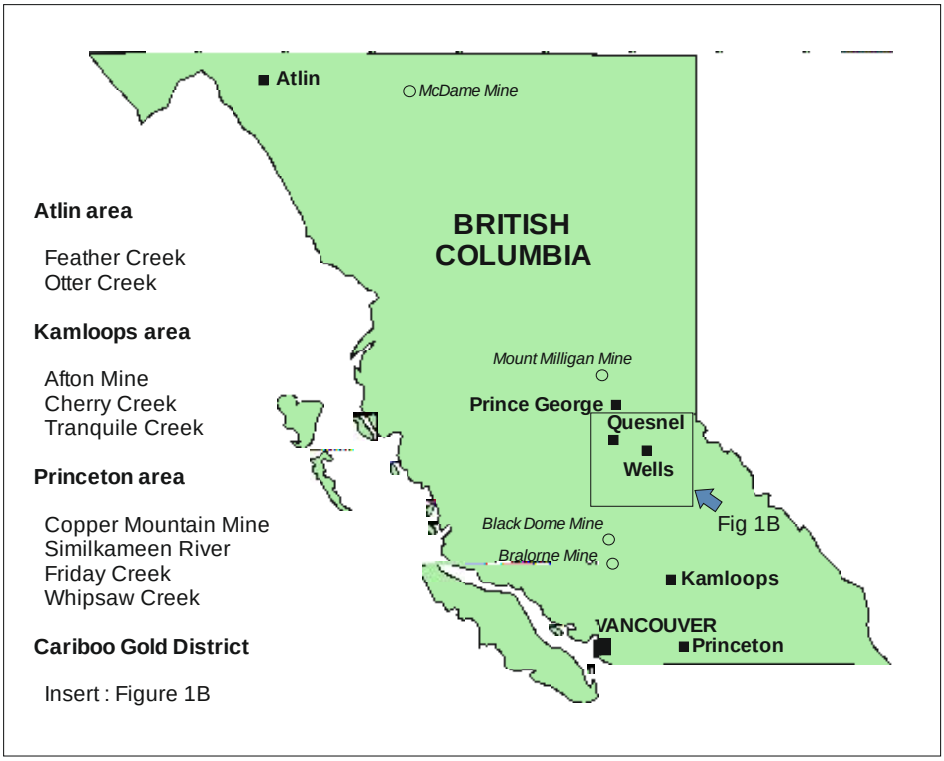

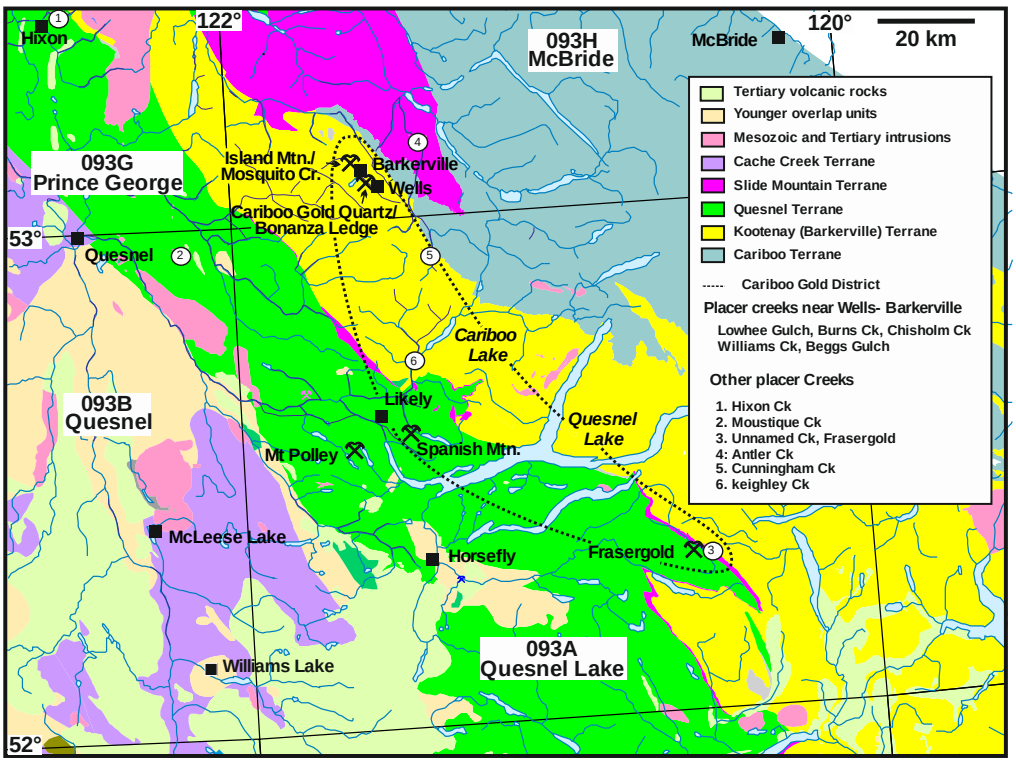

Figure 1. Sample locations in British Columbia, and more detailed locations of samples in the Cariboo Gold District and Environs. Adapted from Mortensen and Chapman (2010).

in alloy composition to refine the characteristics of populations of detrital gold grains. This approach of 'microchemical characterization' has been applied to gold from many localities worldwide, (e.g. Chapman et al. 2000, Potter and Styles, 2003, Chapman et al. 2009, 2017, 2018, with a view to developing a global template by which detrital gold can act as an indicator for the source style of mineralization. The use of inclusions in the characterization process permitted a refinement of placer-lode relationships in the Lone Star area of the Klondike, through discrimination between populations whose alloy composition signatures were very similar (Chapman et al. 2010a,b).

Whilst distinction between populations of grains derived from different mineralizing events and different source styles of mineralization are commonly identified using this approach, the methodology depends upon analyses of much larger gold grain populations than are routinely co-collected in HMC. Such gold grain studies normally require a separate dedicated sampling exercise by personnel experienced in collecting gold particles in areas of low abundance. Any analytical method which could reduce the number of gold grains required to establish provenance would effectively remove this major barrier to using detrital gold as an indicator mineral.

The determination of trace metals by LA-ICP-MS has only rarely been applied to particulate gold, principally because gold commonly contains mercury, which takes considerable time to be flushed through the instrument, and can "poison" it for subsequent use for U-Pb isotopic dating. Unlike many other LA-ICP-MS set-ups available in Canada and elsewhere, the equipment at Leeds is not used for dating by Pb determination, and thus may be routinely employed for gold analysis. The data flowing from LA-ICP-MS analysis would allow characterization of gold based on a far larger array of trace elements than is currently possible using EMPA methods.

The current project involves analysis of populations of gold grains from throughout British Columbia, whose microchemical signature has already been determined. The aims of the project are to provide the first large scale data set which allows:

1. Evaluation of the suitability of LA-ICP-MS for gold analyses
2. Comparison of microchemical signatures with trace element signatures
3. Identification of any trace element signatures diagnostic for gold formed in specific environments.
4. Identification of how elements are distributed in gold grains.

This report contains the findings of this study, which commenced in August 2016. The report determines if LA-ICP-MS analyses can be used to identify gold grain populations from either alkali porphyry or orogenic sources in the study area. It further shows how different elements are found in gold grains, and how this affects the validity of quantitative analyses.

Methodology

Sample Suites

Various sample suites studied in previous projects were available to the present study. These include those which underpinned studies of the Cariboo Gold District (Chapman and Mortensen 2016), and studies of gold derived from alkalic porphyry systems (Chapman et al. 2017). Populations of gold grains previously collected had been mounted in resin blocks and polished to reveal grain core to facilitate earlier microchemical studies. It has not been possible to analyse every grain in all these collections because of the large numbers involved, nevertheless, complete data sets were generated for some sample populations which are considered important to the study. The samples analysed are indicated in Table 1.

Location	No. grains ablated	Area	Affiliation
Similkameen River	118	Copper Mountain	Alkalic porphyry
Whipsaw Creek	47	Copper Mountain	Alkalic porphyry
Friday Creek	54	Copper Mountain	Alkalic porphyry
King Richard Creek	38	Mt Milligan	Alkalic porphyry
Cherry Creek	45	Afton	Alkalic porphyry
Mt Milligan	5	Mt Milligan	Alkalic porphyry
Black Dome	20	South BC	LS epithermal
Hibernia (hypogene)	20	Cariboo gold district	Orogenic
Spanish Mountain (Hypogene)	31		
Hixon Creek	53		
Keighley Creek	16		
Unnamed Creek at Frasergold	8		
Burns Creek	25		
Moustique Creek	27		
Lowhee Gulch	67		
Williams Creek	41		
Beggs Gulch	29		
Lower Antler	16		
Upper Chisholm Creek	20		
Dragon Creek	25		
Cunningham Creek	22		
Bralorne	7	South BC	Orogenic
Ruby Creek	17	Atlin	Orogenic (?)
Feather Creek	17	Atlin	Orogenic (?)
Mc Dame	5	North BC	Orogenic

Table 1. Location of the different placers and the associated style of gold mineralization

Analytical Method

Images of the polished block surface were used to identify each grain within each sample population and this permitted correlation of historical micro-chemical data with the new information obtained by LA-ICP-MS.

For quantitative analysis, the LA-ICP-MS system uses an Agilent 7500c quadrupole mass spectrometer, combined with a Geolas ablation system to determine the composition of individual grains. The Geolas ablation system uses a Compex 103 ArF excimer laser at a wavelength of 193nm, delivering an energy density of up to 20 Jcm^{-2} on the sample surface at a pulse frequency of up to 20Hz with spot sizes from 5µm to 160µm. The ablated material is transported from the ablation cell to an Agilent 7500c ICP-MS using 99.9999% He flowing at 2 ml min^{-1} into a cyclone mixer where it was combined with the Ar carrier gas flowing at 1.02 ml min^{-1}. The instrument can be operated in reaction cell mode using 2.5 ml min^{-1} 99.9999% H_2 to remove interferences from ^{40}Ar on ^{40}Ca and from ^{56}ArO on ^{56}Fe, however this also reduces the signal intensity of both the background and the analyte. In general, the target elements analysed had low background signals and the only benefit would have been the ability to use the major ^{56}Fe isotope for analysis, but is was found that operating without the reaction cell allowed better observation of the ablation of elements at low concentrations.

Figure 2 shows the effects of ablating gold grains by 150 laser pulses. The predominant feature is the lip of metal that has condensed on the surface around the ablation pit. This is much less than the volume of material that has been transported into the ICPMS, but analysis of these rims does not indicate there has been any elemental fractionation between what has been transported and what has been condensed. As gold is easily ablated, the laser energy was reduced to 6 Jcm^{-2} on the surface at a pulse rate of 5 Hz because at higher energies or higher pulse rates gold particles were ablated all the

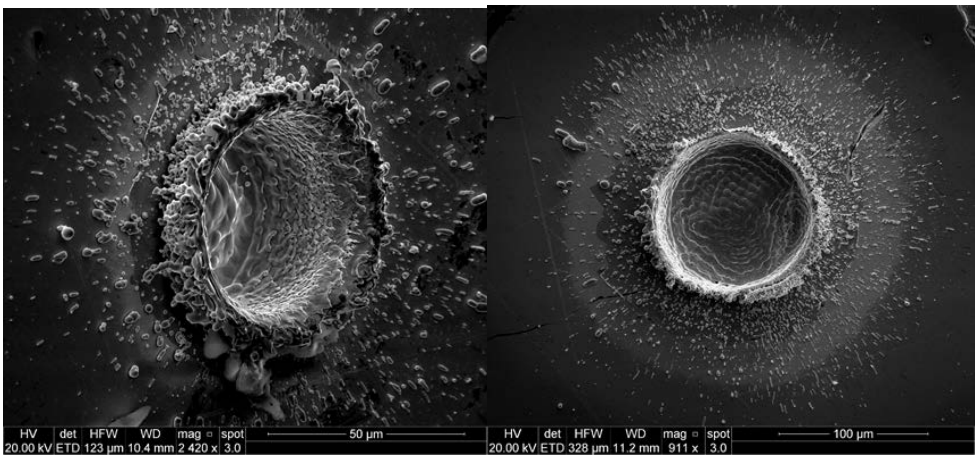

Figure 2. SEM images of laser ablation pits about 50 µm deep in gold after ablation for 150 laser pulses. Cooled metal forms a rim around the ablation pit, but the majority of material is transported to the ICPMS.

way through too quickly. The lower energy did result in a lower signal but this was not overly significant.

The choice of laser spot size was established through experimenting with spot diameters between 5 and 100µm. Smaller spot sizes resulted in loss of signal with progressive ablations because laser energy could not penetrate to the bottom of the holes and hence ablation ceased. All the grains were analysed with spot sizes of between 25-100 µm, most commonly 50µm.

In addition to a single spot analysis of each grain using the quadrupole system, the project gained access to a LA-ICP-MS ToF apparatus in which the concentration of all elements are measured simultaneously. This methodology generates elemental distribution maps at the trace level. The technology has recently been developed by TOFWERK of Thun, Switzerland and comprises a iCAP RQ the Thermo Scientific ICP-MS where the quadrupole mass filter is replaced by ToF mass filter, ion transport and detection system. Whereas quadrupole systems measure element sequentially and spends only a small percentage of the cycle time on the selected isotopes, the ToF system measures from ^{6}Li to ^{238}U in 30ms. Combined with a fast wash out ablation cell system produced by Teledyne Ceetac Technnologies the low dispersion of material ablated (~10ms at FWHM) allows laser repetition rates of up to 100Hz to be used with minimal overlap from the adjacent laser pulses. Element maps were generated using adjacent individual laser pulses of 5 or 10µm. At a resolution of 5µm individual spots we were able to traverse 100µm per second without overlap of individual pulses.

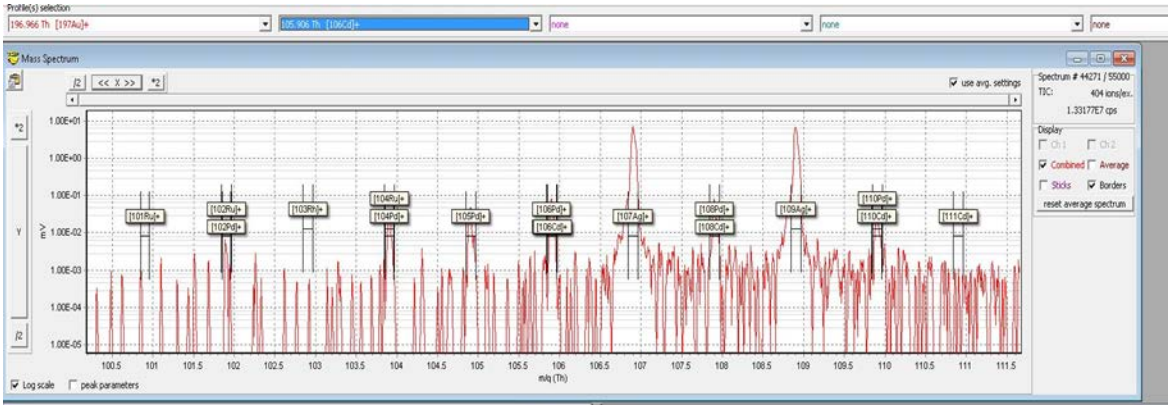

Figure 3. Example of the mass resolution of the ToF mass spectrometer which shows the isotopes detected over a 10 amu mass range. The instrument is capable of detecting isotopes from ^{6}Li to ^{238}U. The isotopes chosen here were usually the main isotope, but also isotopes which were free from the isotopic interference of other elements, examples of which can be seen here.

An example of the area of a mapped gold grain is shown in figure 4. The speed of data acquisition, resolution, elements acquired and the detection limit is far superior to LA-ICP-MS quadrupole systems currently used to produce element maps in different minerals. For example a 500 x 500µm area ablated at a resolution of 5µm produces 10,000 laser analysis spots in approximately 8.5 minutes for every isotope above the limit of detection. It was only possible to analyse a small number of gold grains using this equipment, but the resulting data proved particularly informative.

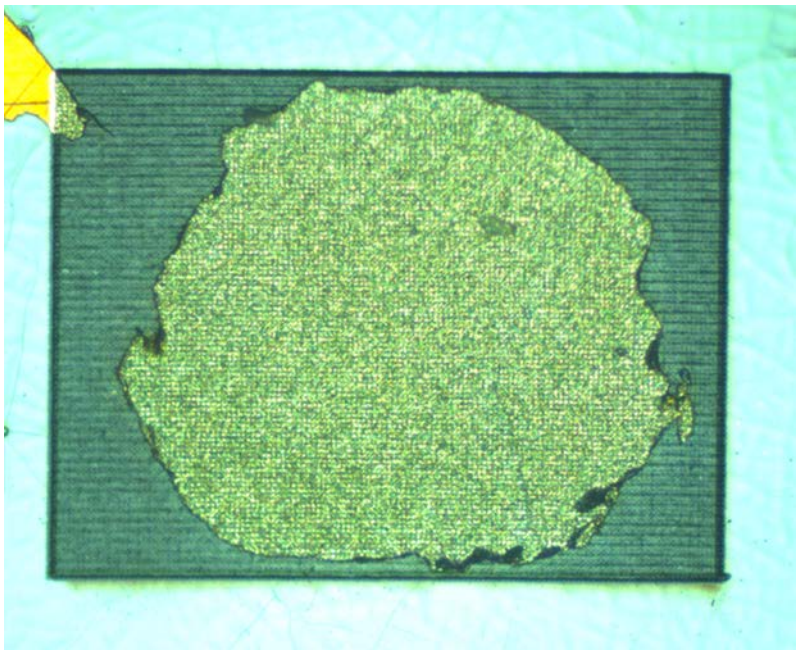

Figure 4. Reflected light image of a gold grain that has been ablated with a succession of 5µm laser spots. The close spacing and small ablation spot ensures the best resolution currently possible. In the top left is part of a grain that was within the area ablated showing the difference pre- and post-ablation.

Calibration and Quantification

The gold grains were analysed for a large number of elements to permit a comprehensive appraisal of which could i. form useful discriminants for the identification of gold grains from different deposit types, ii. potentially indicate processes operating during precipitation. The suite of elements was Si, Al, S, Ti, V, Cr, Mn, Fe, Co, Ni, Cu, Zn, Ga, Ge, As, Se, Y, Nb, Mo, Rh, Pd, Ag, Cd, In, Sn, Sb, Te, La, W, Pt, Au, Hg, Pb, Bi, Th, U. LA-ICPMS requires that elements are measured as ratios relative to an internal standard element which is usually the element with the highest concentration, and consequently all elements were measured against Au as the internal standard. Integration of the standard and sample signals was achieved with the SILLS software package (Guillong et al. 2008). The London Bullion Market Association Reference Standard AuRM2 was used as the primary standard for Ag, Al, As, Bi, Cr, Cu, Fe, Mn, Ni, Pb,

Pd, Pt, Rh, Sb, Se, Sn, Te and Zn with the additional elements calibrated against NIST 610, again using Au as the internal standard element. However, AuRM2 was not suitable for the accurate determination of the Ag/Au ratio, as the Ag/Au of the standard is 9.96^{-5} whereas most of the gold grains have Ag/Au ratios of 0.25 to 0.66 (corresponding to ratios of 80:20 to 60:40 wt. percent Au to Ag respectively). Use of this standard would require extrapolating the calibration many orders of magnitude above the value of the standard, whereas the NIST 610 standard has a Ag/Au ratio of 0.106, which is closer to the sample values. The Ag/Au ratio used in the final quantification used NIST standard 481, which is a set of Au-Ag wires ranging in composition from pure Au and Ag to intermediate compositions of 80:20, 60:40 and 40:60 wt percent Au:Ag respectively. The 80:20 standard was used for quantification and despite the difference in matrix and in the concentration of both elements gave a calibration that was almost identical to that obtained using NIST 610. The calibration for Hg was established using the USGS synthetic sulphide standard MASS-1 as Hg is not present in NIST or the AuRM2 standard. In this instance the calibration was based on using Ag as the internal standard element as there is no Au in MASS-1 and manual extraction of the counts per second ratio for Hg/Ag from the SILLS output to use with the Hg/Ag wt/wt ratio of the standard. A combination of calibrations based on the S/Au from NIST 610 and S/Ag from MASS-1, (the calibration procedure was the same as for Hg/Ag), was used to determine the S weight/weight ratio in the gold grains. However, because of the poor response of S the values they were used as indicative only.

SRM-610 and AuRM2 were used to check for instrumental drift, which was found to be insignificant over each day's analysis. The slope of the calibration graphs converting the counts per second ratios to weight ratios was consistent over the 2-3 week period during which analysis was carried out indicating the stability of the instrumentation. Using SILLS it was possible to determine the wt/wt ratios of element using either NIST 610 as the calibration standard or alternatively AuRM2.

The reproducibility of major element data from electron microprobe analyses and LA-ICP-MS data was established by comparing data describing a populations of gold grains derived from epithermal and akalic porphyry environments. Analyses for the major alloy elements, Au, Ag, Hg and Cu, are presented in figure 5. The data exhibit near identical median values and the same range of concentrations. The main difference is the Cu data from the epithermal gold where the probe data are an order of magnitude greater than the LA-ICP-MS data, however, this is an analytical artefact resulting from the analytical values being close to the limit of detection of the probe, which is typically 200ppm. When the Cu concentrations in the grains are higher both methods of analysis give the same results.

The data from LA-ICP-MS (ToF) has been presented as elemental intensity maps rather than concentrations as this is the easiest way to visualize the distribution of elements in the gold grains. The element concentration maps are generated by calculating the intensity of each element relative to Au for

each pixel. It would be possible to convert these values to concentrations using the same approach as for the analyses form the quadrupole system, but this process is extremely time consuming and was not warranted in this study.

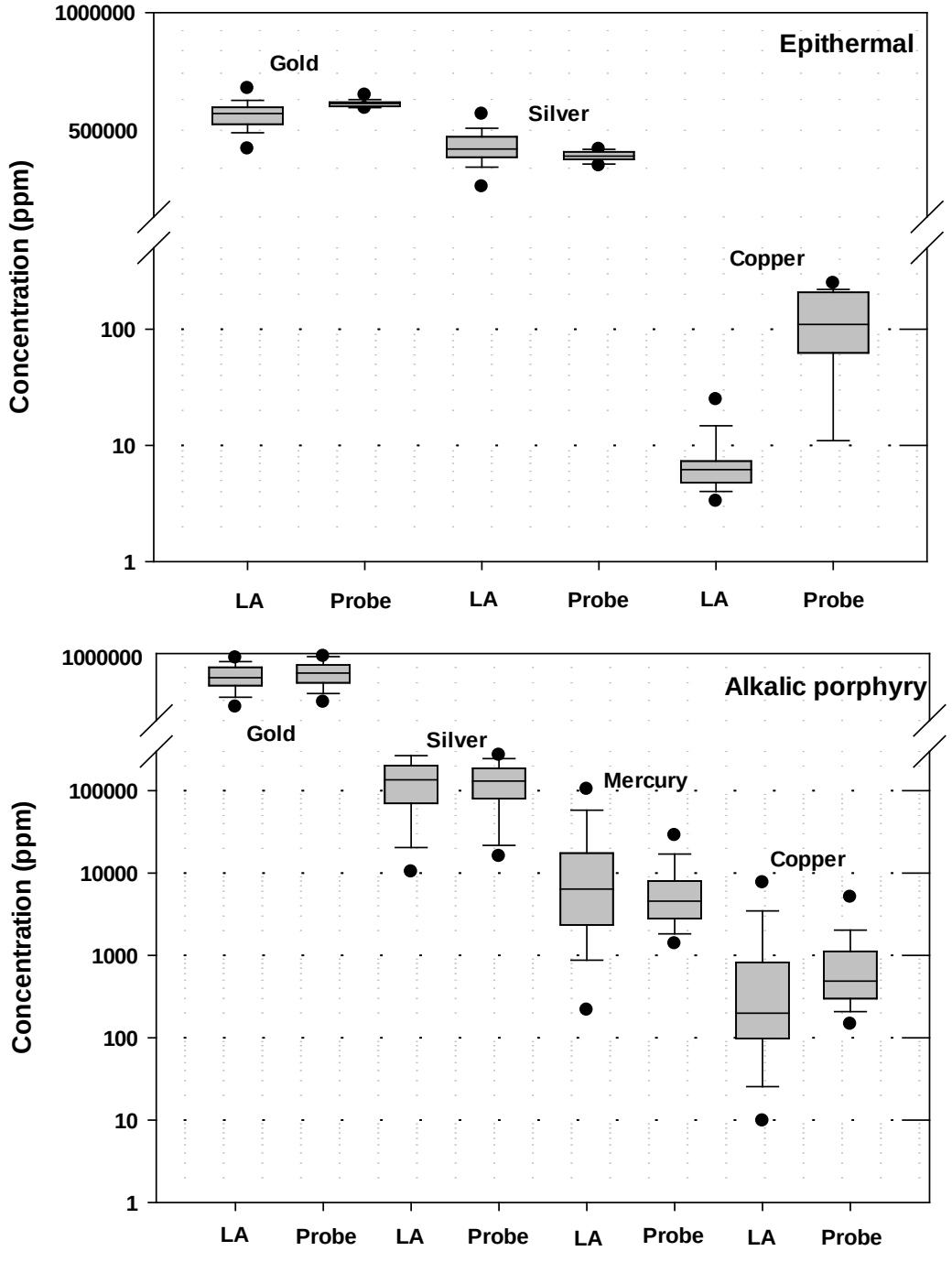

Figure 5. Comparison of the major alloy elements in gold grains from two different placers to assess the comparison between Electron Microprobe Analyses and LA-ICP-MS analyses.

Results

LA-ICP-MS Quadrupole Analyses of Gold Grains

Over 800 gold grains were analysed using the quadrupole system in Leeds. The sample locations are provided in table 1 and comprise five placer localities associated with alkalic porphyry systems and eighteen placer localities associated with orogenic gold. Grains were also analysed from one epithermal locality, (Black Dome), but it is not possible to develop any generic statements regarding the compositional characteristics of epithermal gold based on a single occurrence, and therefore this report is concerned primarily with distinctions and similarities between gold derived from alkalic porphyry and orogenic sources. Figure 6 compares analyses of gold grains from alkalic porphyry and orogenic mineralization, and indicates the degree of variability in analyses for specific elements. For the majority of the elements there is at least an order of magnitude variability of the concentration at the 25^{th} to 75^{th} percentile range and much more than that for all the data acquired for each element. There are clearly inclusions of different minerals, (se later discussion), with pyrite being the most common. A range of other elements are associated with the pyrite. The size and number of any inclusions ablated will influence the overall analysis. Therefore the concentration of elements determined is only representative of the cylinder of material ablated and the relationship of this value to the composition of the whole grain is unknown. Only by dissolving and analysing whole gold grains can the true composition of each grain (i.e. alloy plus inclusions) be obtained. However, analysing a sufficiently large population of grains from the same placer source will alleviate this potential bias.

The elements Ti, V, Mo, Pd, Cd, In, La, Hg, Pb, Bi (shown in red in figure 6) all have a median value that is at least x10 greater in gold grains derived from alkalic porphyries. In addition the average value, (which is influenced by the greater abundance of inclusions in alkalic grains), is higher for most of the elements analysed as is the absolute maximum concentrations. Figure 7 shows variation between the signatures of sample populations from three placer populations collected in the environs of Copper Mountain in terms of the trace elements, whereas the Hg and Cu values are broadly comparable.

LA-ICP-MS Analysis of Inclusions in Gold Grains

When ablating the gold grains, areas where inclusions were exposed were avoided. However, as the laser ablated beneath the surface inclusions were encountered and these influenced the analytical output according to their size. Figure 8 shows the ablation profile of a gold grain that contains only the Au alloy elements and a large pyrite inclusion that was encountered beneath the surface of the gold grain. A total of eleven other elements were recorded once ablation of the pyrite commenced, which shows that the

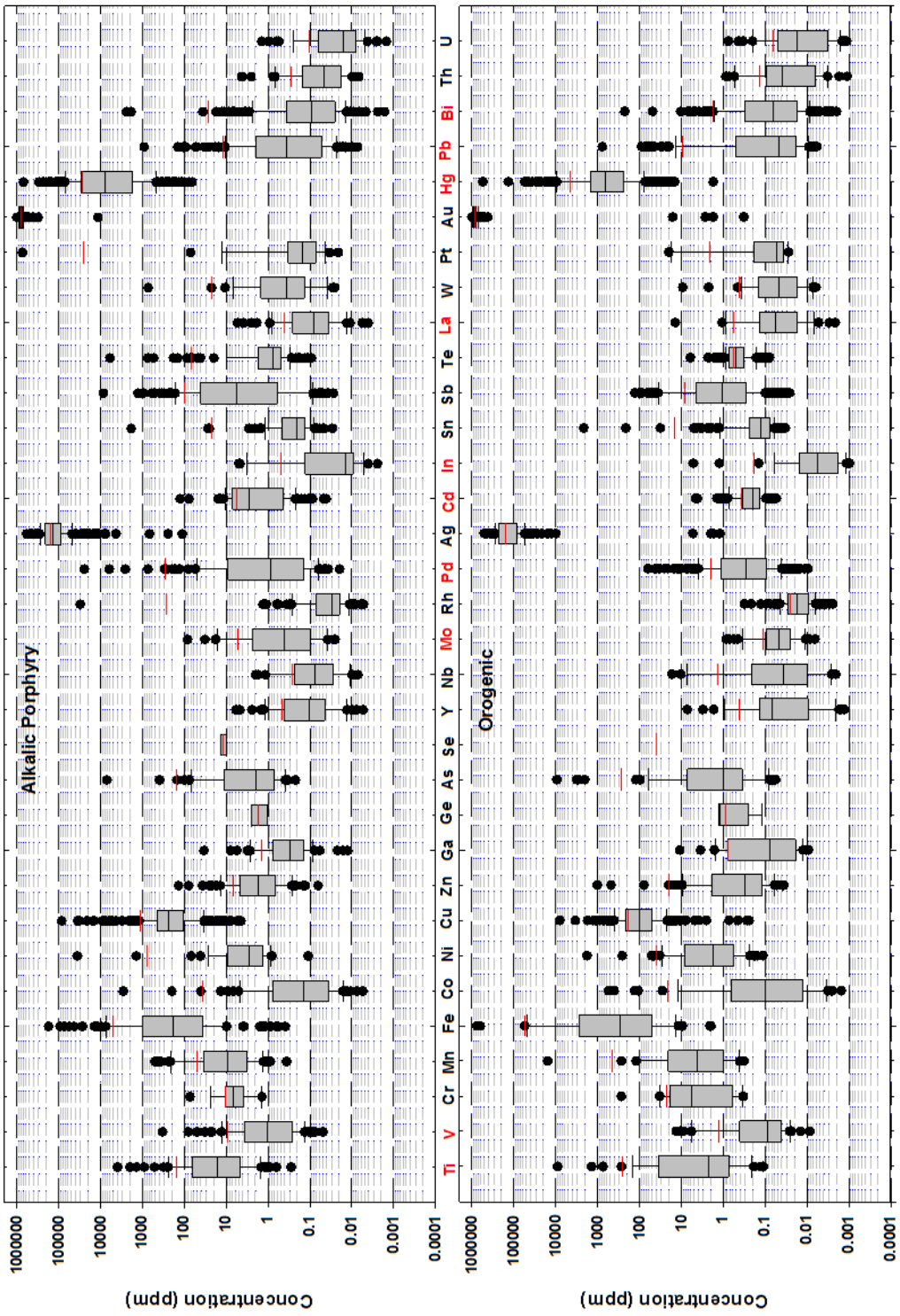

Figure 6. Analyses of all gold grains from alkalic porphyry and orogenic mineralization as box (25th and 75th percentile) and whisker (5th and 95th percentile) plots with outliers. Horizontal black line is the median value and the red line the mean value.

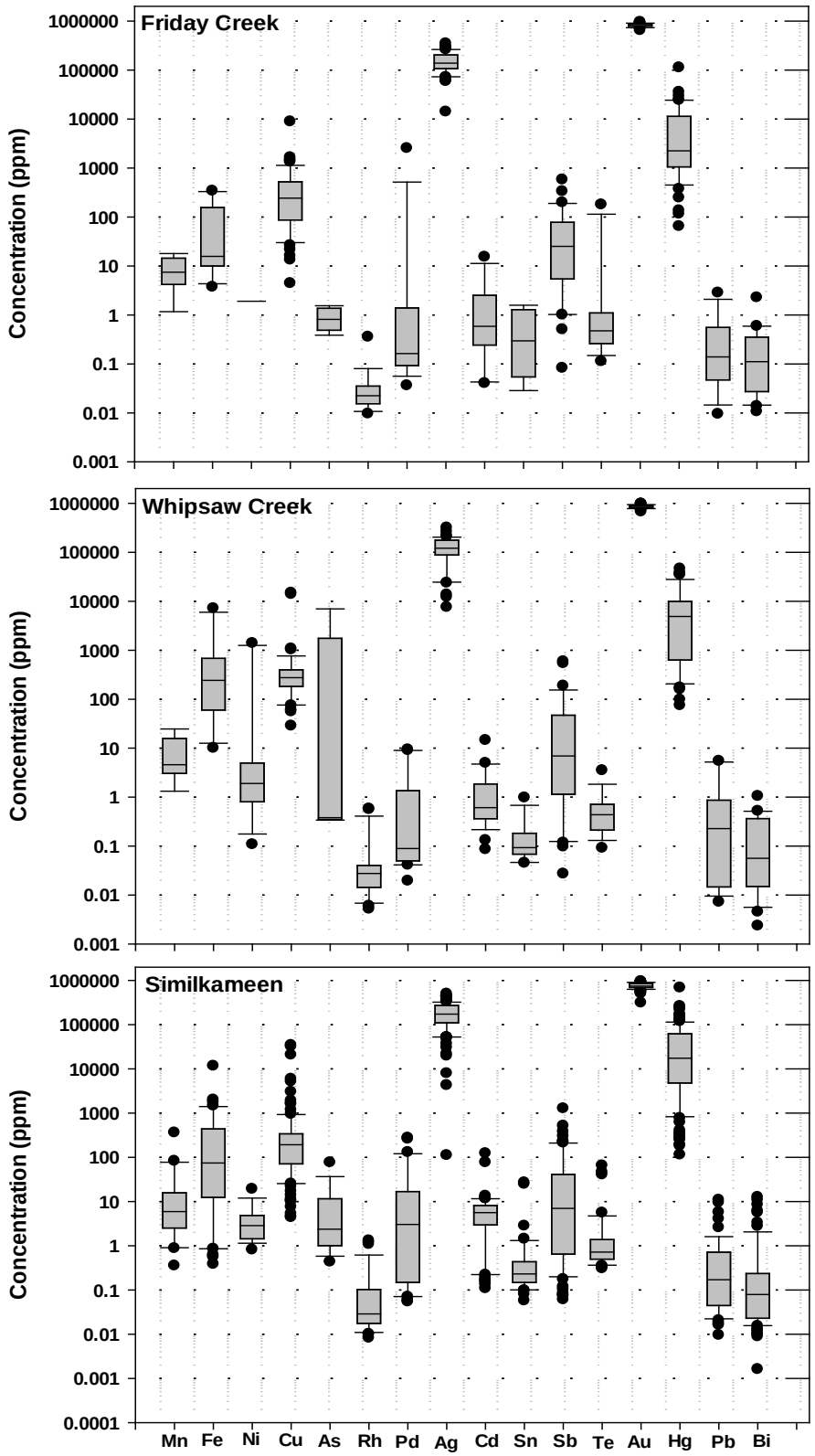

Figure 7. Placers from different streams related to the same alkali porphyry source (Copper Mountain porphyry) illustrating the variability of analyses due to the presence of inclusions.

pyrite exhibits a trace element profile distinct from the gold. In cases like this, the part of the signal that is due to the composition of the gold alloy is processed separately to the inclusion. Large inclusions are obvious, but many are smaller, and while they contain the same additional elements processing the analytical output is more challenging, because the absolute values for the concentrations of elements within the inclusions are dependent on the size of the inclusion analysed. This varies according to the volume of the gold grain analysed and may not be directly comparable from one grain to another. In addition, when ablating small inclusions some elements may not be recorded at all, as the Quadrupole ICP- MS measures elements sequentially, and the mass of the inclusion bay have passed through the ICP-MS before all elements are measured.

In figure 9 the elements occurring in pyrite inclusions from the alkalic porphyry and orogenic placers are presented as percentages relative to Fe at a nominal value of 100%. From the analysis of gold grains that have no inclusions and contain only the alloy elements (as in figure 8 left profile) there is no recorded signal for Fe. Therefore, a Fe signal recorded together with other elements that are not present when only the gold alloy is ablated is indicative of an inclusion. This assertion is confirmed in the ToF-MS images of gold grains which show that Fe is only present as occasional large inclusions and many smaller ones, but is not part of the gold alloy. Figure 9 shows that many of the elements have similar ranges and median values irrespective of whether the gold grain was derived from an alkali porphyry or an orogenic deposit, but others such as Cr, Zn, Mo and Rh differ.

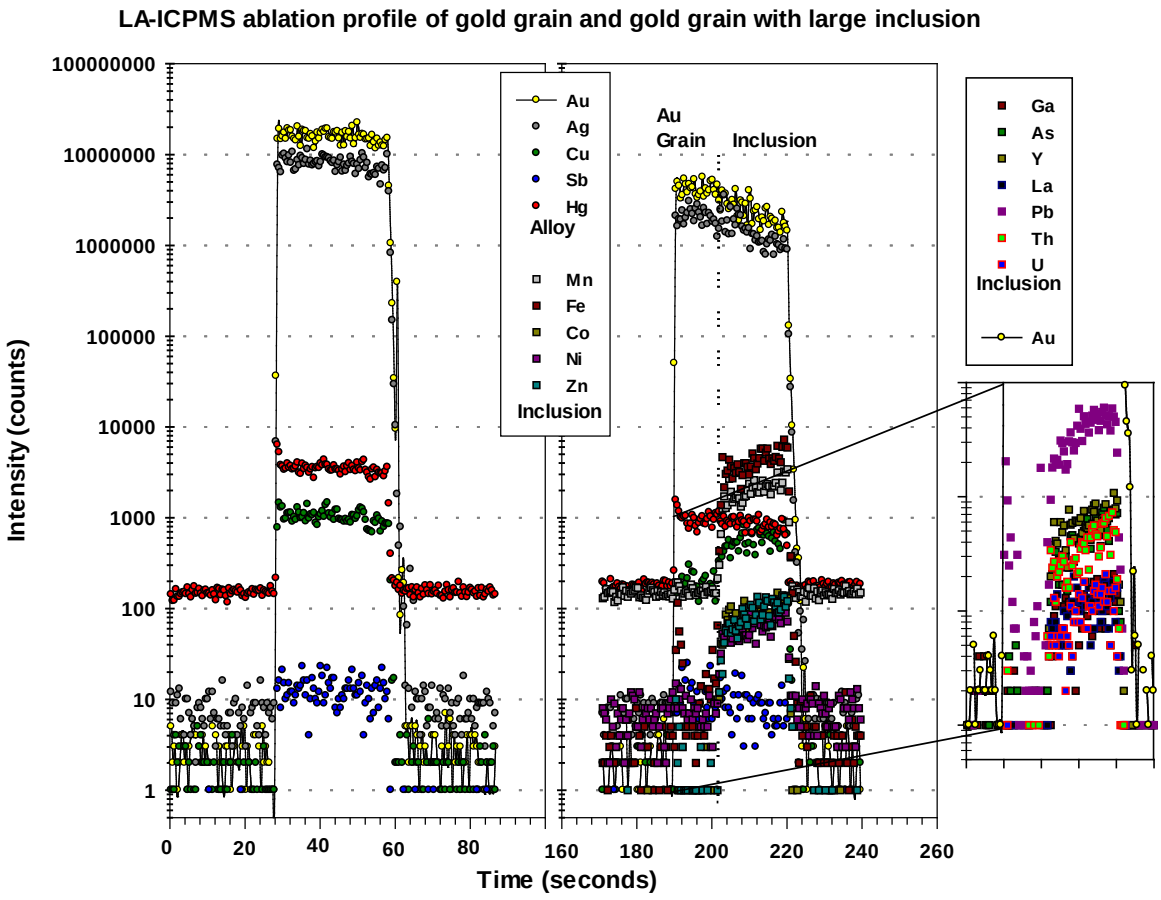

Figure 8. LA-ICP-MS profiles from the ablation of 2 gold grains. On the left only the gold alloy was ablated, no inclusions were present, and Au, Ag, Hg, Cu and Sb are parallel to each other. On the right the gold alloy was ablated but deeper in the grain a pyrite inclusion was co-ablated, and consequently the trace reflects the alloy, the inclusion and the inclusion trace element signature.

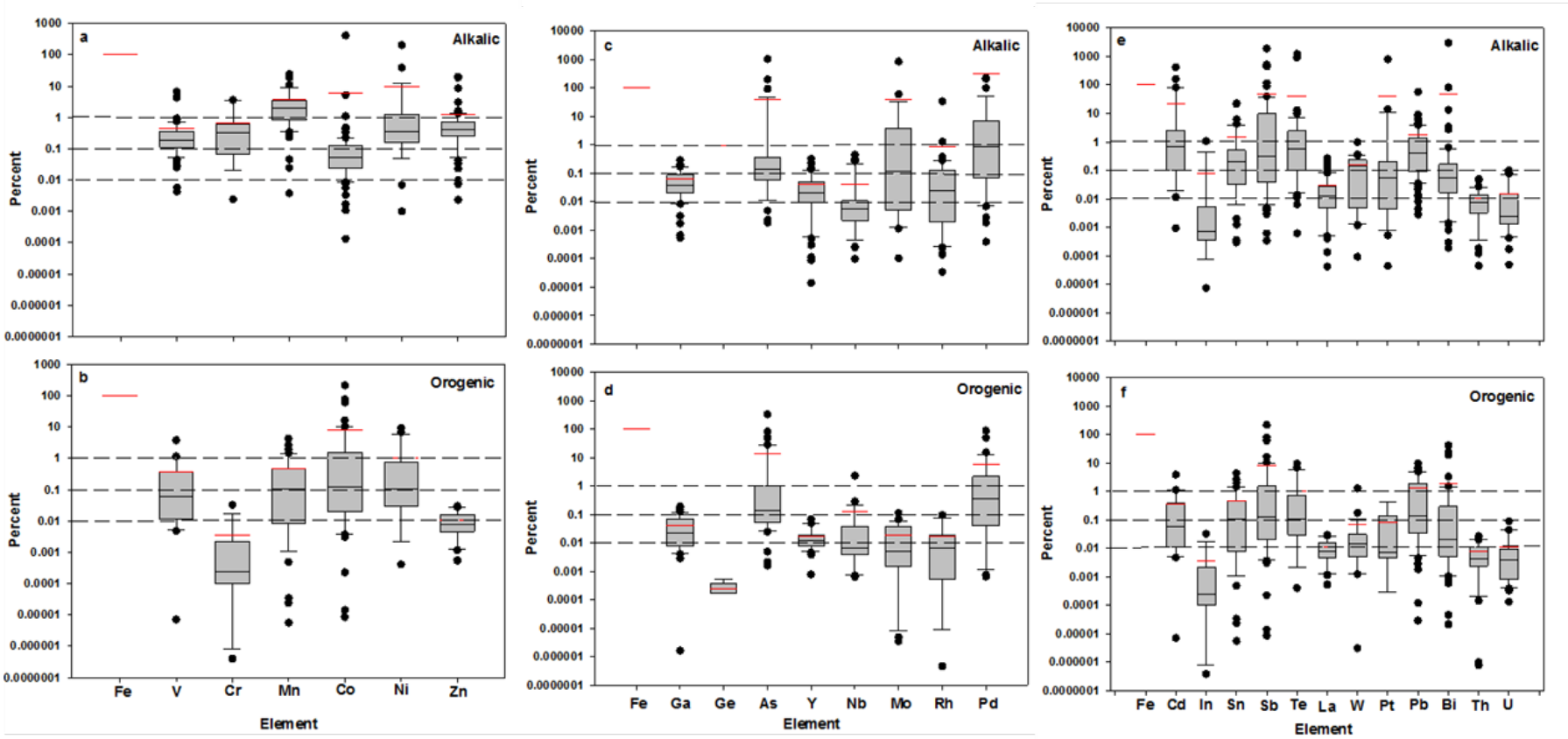

Figure 9. Trace elements in pyrite inclusions in gold derived from alkalic porphyry and orogenic deposits calculated as a percentage relative to 100% Fe. The pyrites were encountered during ablation of the gold grains i.e. below the surface. Some elements have outlier values, some over 100%, that indicate inclusions other than pyrite were present within the cylinder of material ablated. Using the 25th to 75th percentile range (grey box, horizontal black line is the average and red is the median) to discriminate between gold from alkalic porphyry and orogenic settings, the elements Cr, Mn, Zn, are the only ones higher in the alkali deposits compared with the orogenic. However, using the 95th percentile and high outlier values, gold from the alkalic porphyries exhibit higher concentrations.

LA-ICP-MS Time of Flight Analyses

Time of flight data was used to illuminate the variable concentrations and the heterogeneity of concentrations recorded in the LA-ICP-MS (quadrupole) analyses. As the quadrupole-MS data is rely only the analyses of the portion of the grain ablated it is essential to understand how representative this is to the analyses of the whole grain. Only Au, Ag, Cu, Hg $\pm$ Sb exhibit generally homogeneous distribution consistent with association with the Au alloy, whereas the distribution of other elements is more random. The presence of micron size inclusions of different elements and minerals can be seen from SEM imaging but this is only a 2-D view and very much smaller inclusions may also not be observed. LA-ICP-MS analyses records the presence of elements at sub ppm levels that are not observable as inclusions.

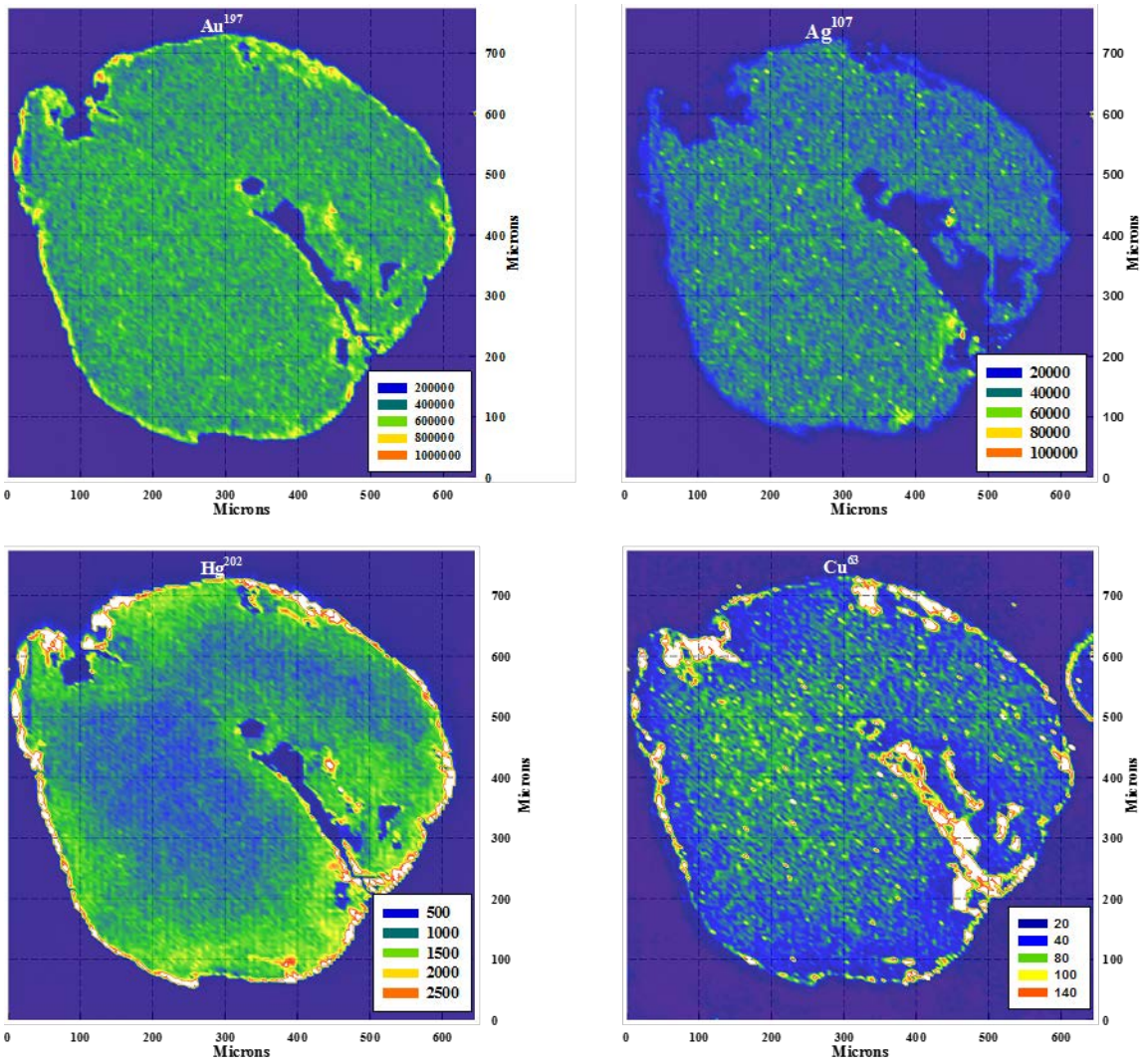

Figure 10. LA-ICP-MS(ToF) intensity maps for Au, Ag, Cu and Hg in a placer grain from the Similkameen River. The image is made from the indicated isotopic intensities measured for each 5μm laser pulse. Each image represents 19,500 laser pulses.

Figure10 shows the element intensity maps generated by the ToF system for the main alloy elements in a gold grain from the Simalkameen River. These images are constructed from 19,000 individual 5μm laser shots. The Au and Ag distribution is homogeneous over all of the grain, except for the grain edge, where there is a higher gold intensity is coincident with a lower Ag intensity. This is a well known effect in many placer grains where there is dissolution and re-precipitation of an essentially pure gold rim. Both Hg and Cu exhibit a sharp increase in concentration at the grain edge and a more gradual increase away from the grain centre towards the edge. Therefore it is obvious that the position of analysis will affect the result, in this case by a factor of 2 or 3. Analysed of grains by LA-ICP-MS (quadrupole) involved positioning the laser beam as close to the grain centre as possible as this is where the analyses would be least affected by the heterogeity described above.

In figure 11 other selected elements from the same grain are clearly heterogeneously distributed. The large non-gold grain areas are due to the presence of Fe (pyrite) which also contains Cu at concentrations above those in the gold alloy. By adjusting the concentration range in figure 11, the variability in the background Cu signal can be reduced to show that small variations in concentration within the alloy are present. The image for Pd (figure 11) is another example of the low but heterogeneous concentrations that can be observed with the ToF system. There are a number of spots with a signal that is significantly above the limit of detection and these are interpreted to represent sub-micron inclusions. Inclusions of three other elements, Sb, Bi and Pb, are also shown in figure 11. The inclusions are quite numerous in this section and overall may constitute a small but significant contribution to the trace composition of the gold grain. The ability of the TOF system to measure all elements simultaneously allows us to see that Sb, Bi and Pb, are most often located at the same point in the gold grain. This information would not be obtainable with a quadrupole-MS system because of the sequential mechanism of acquiring data. In the gold grain illustrated in figure 11, Sb and Bi always correlate, but there are some Pb signals that do not correlate with these two elements and these probably indicate galena inclusions.

The grain shown in figure 12 is also from the Similkameen River placer and when compared with the grain illustrated in figure 11, illustrates the grain to grain variability from the same placer locality. In this case the Ag intensity is not homogeneous and when calculated as ppm ranges from c. 2% to c. 13%. The highest iodine (I) intensities usually correlate with the areas of highest Ag intensity. There is also an individual inclusion where the highest I intensity is observed. The presence of I was one of the unexpected discoveries for which there is no explanation at this stage. In the grain illustrated in figure 11, Pd was restricted to discrete inclusions, but in figure 12, the areas of highest intensity are associated with Au alloy in the centre of the grain, and become gradually lower towards the edge.

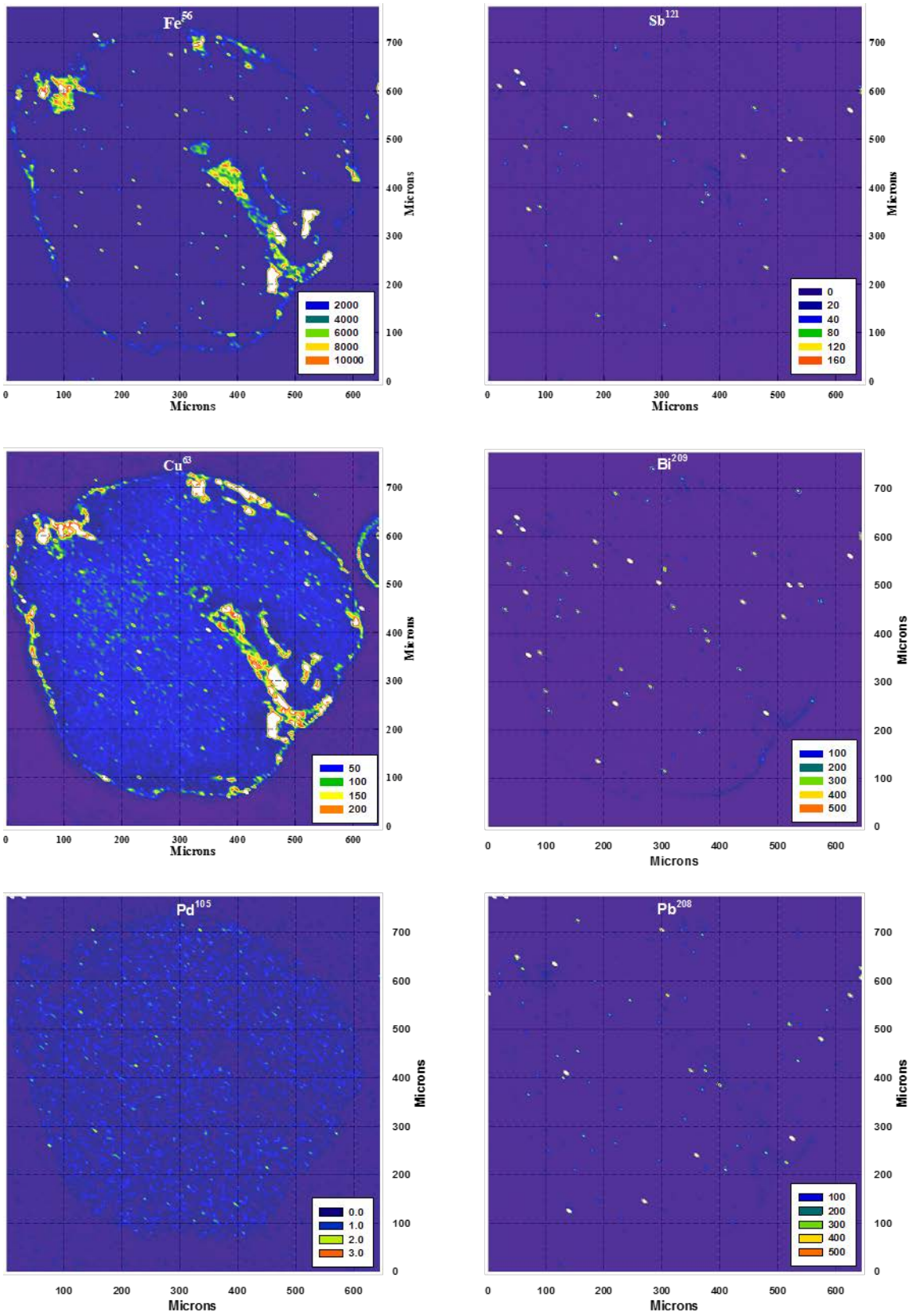

Figure 11. Selected elements to show the heterogeneous distribution of trace elements in the gold grains. Note the presence of a large pyrite and the many smaller pyrite inclusions. Sb, Bi and Pb are all present as inclusions and correlate with each other. Same grain as figure 10.

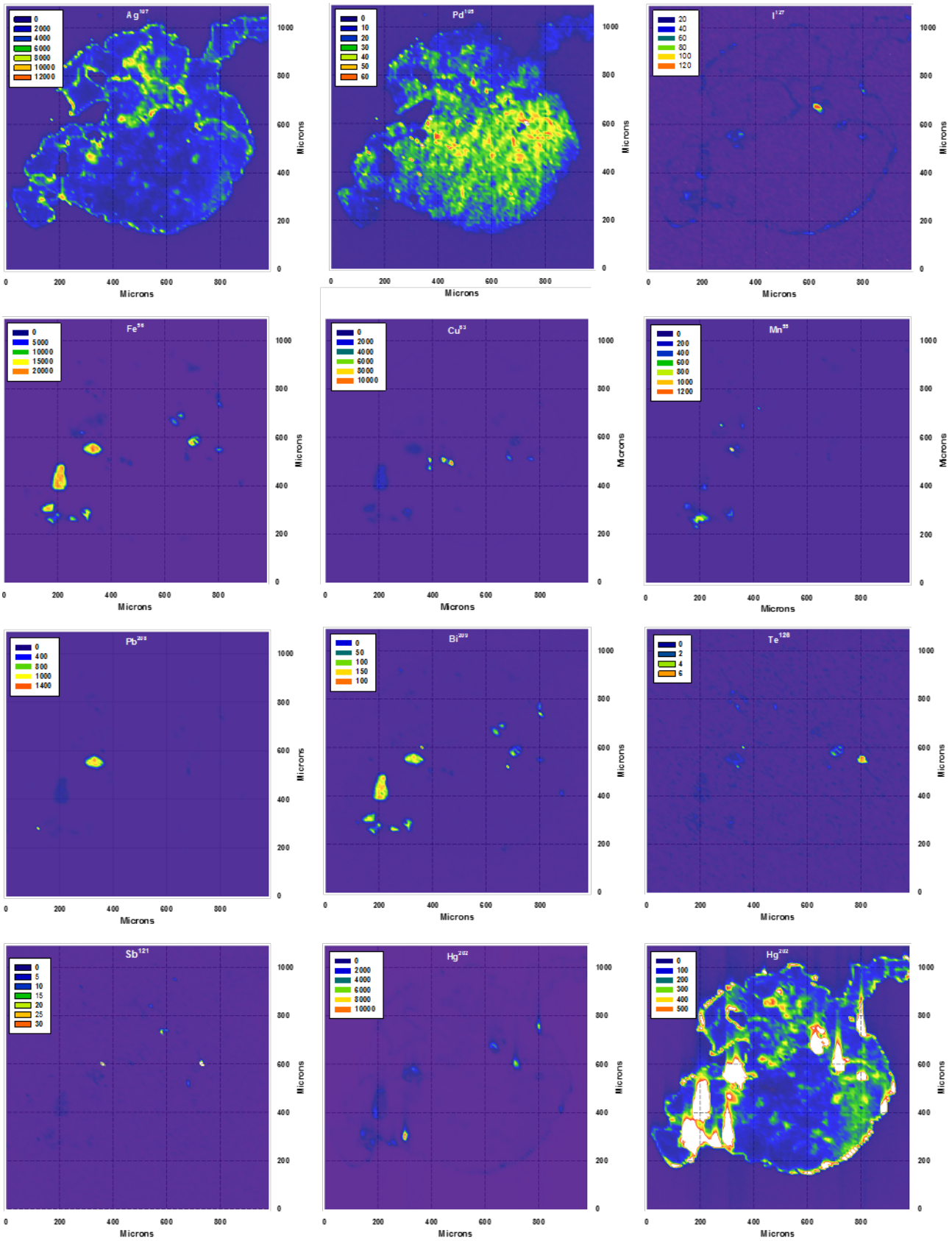

Figure 12. Grain from Similkameen River with heterogeneous Ag and Hg also present as inclusions. Pyrite, Cu and Te-bearing inclusions present together with Fe-Pb-Bi and Fe-Bi-Sb associations. Iodine is associated with high Ag concentrations and as an individual inclusion.

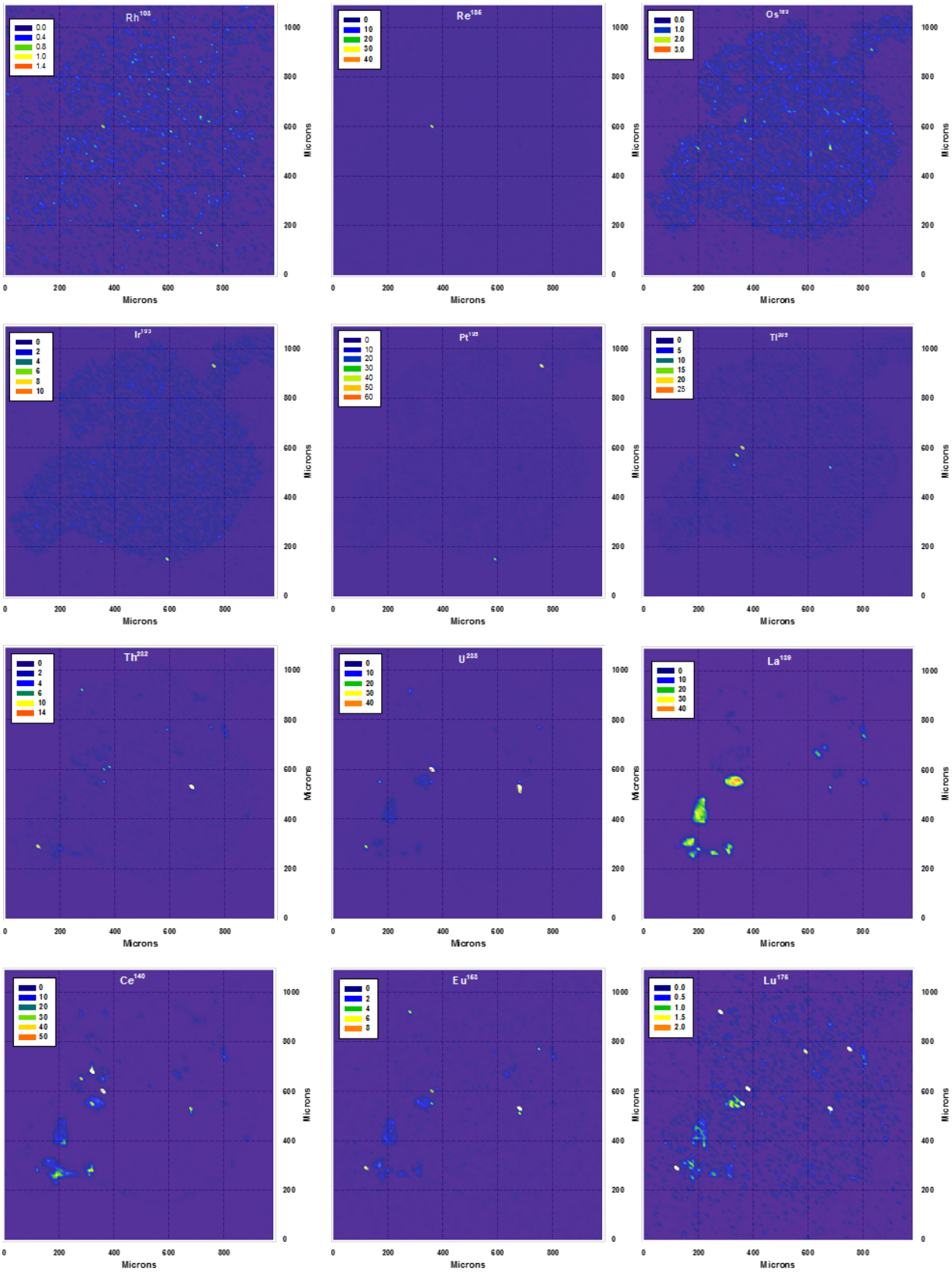

Figure 13. Additional trace elements as inclusions in grain illustrated in figure 12 . REE associated with the pyrite. Rh-Re-Os-Tl, Pt-Ir and Th-U correlate as small inclusions.

In these grains inclusions a few microns to tens of microns can be observed optically. Pyrite is most common, with chalcopyrite and galena also present. In figure 12 several areas of high Fe intensity are present which correlate with lower intensity of Bi. Lead is also present and correlates with one area of Fe concentration but not others. There are 4 high Cu intensity areas and some lesser ones but these do not correspond with high Fe and so the inclusions are not chalcopyrite. There is also some degree of correlation between Te, Bi, Pb and Fe. There are areas of high Hg intensity and Hg has shown to reach 10% in some grains from alkalic porphyry placers. By setting the upper intensity level to a lower value the overall distribution of Hg becomes more apparent and shows a strong correlation with areas of high Ag and I. The areas with the highest I intensity correspond with the areas where the large Hg inclusions are present.

In figure 13, element intensity maps are presented for some of the more unusual elements, which illustrates the range of elements present within the gold grains. The intensities for these are low because they are very small inclusions (based on some approximations they would be less than 100nm) but they generate signals above the limit of detection. There are distinctive small inclusions containing Rh which correlates with the one inclusion of Re and one of Os. The two inclusions of Pt and Ir correlate as do inclusions of Tl, Th and U. Finally four intensity maps for some REE, La, Ce, Eu and Lu are presented which indicate an association with Fe and presence as discrete inclusions. In the data from the ToF all the REE were detected but only some representative ones are shown. The ability of ToF-MS to record these elements from extremely small inclusions exemplifies just how powerful a technique this is compared to quadrupole-MS.

Time of flight-MS provides much more information than has previously been possible using the quadrupole system because the images of elemental distributions provide detailed information at higher spatial resolution. Figures 11 and 12 show intensity maps for 23 different elements, but more than 30 elements have been detected in total. The correlation of different groups of elements based on their properties might be predictable, but the presence of so many elements in gold grains was not anticipated. The drawback with the ToF approach is the time required in data processing to convert instrument outputs to elemental maps.

Discussion

Differentiation of gold from alkalic porphyry and orogenic hydrothermal systems

The datasets describing Au compositions show compositional differences between populations of grains derived from alkalic porphyries and orogenic systems. It is immediately apparent that the analyses of one or even a few gold grains is not sufficient to characterize a population of grains, and determination of source type could only be achieved by analysing a much larger representative population. It is not possible to predict the number of grains required, because the amount of intra-grain and inter- grain compositional variation is not known at the outset.

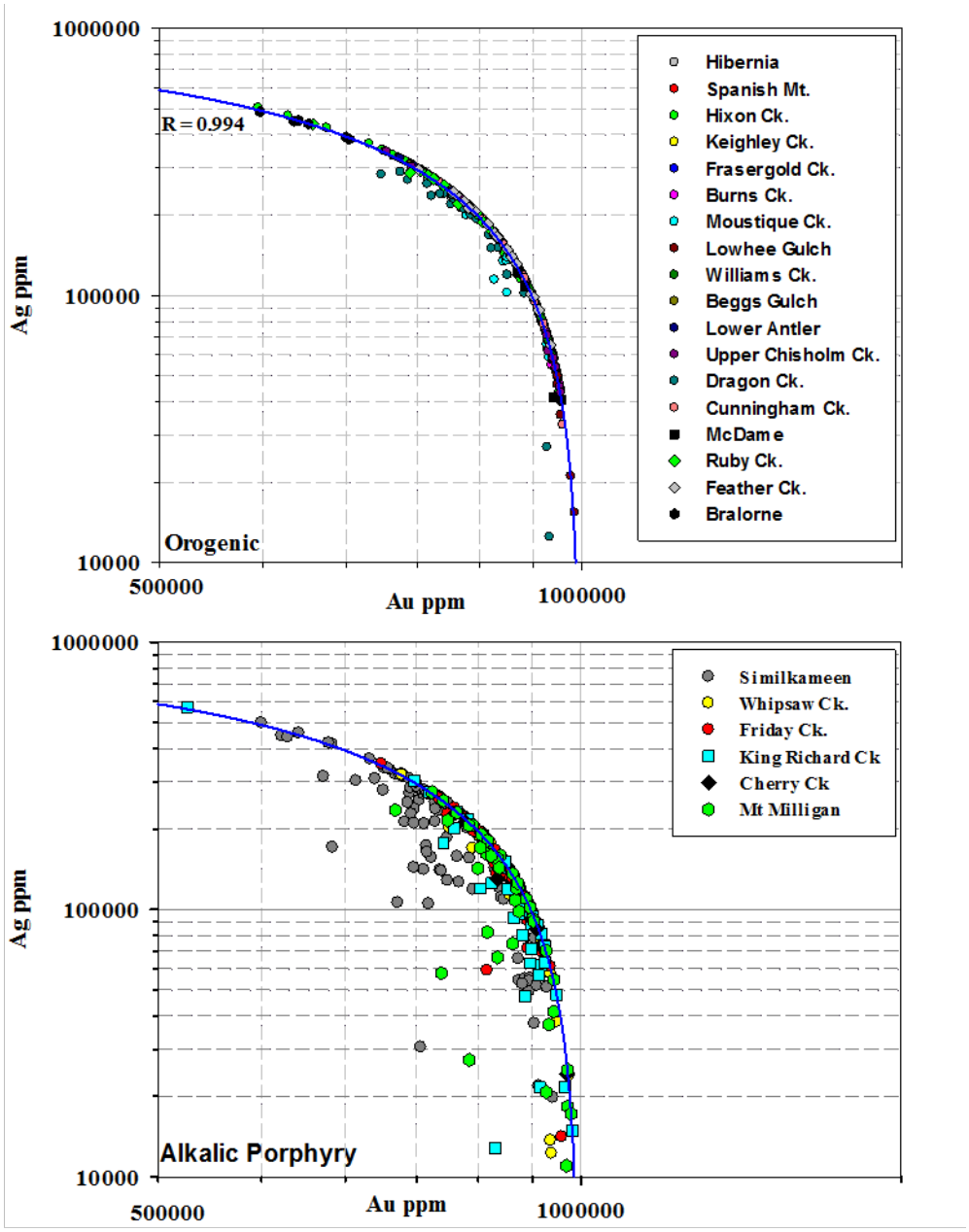

Figure 14. LA-ICP-MS analyses of Au and Ag in grains from each deposit studied. Orogenic deposits plot along a binary mixing line with very little deviation. Many grains from the alkalic porphyry associated placers also conform to this relationship, but others deviate, principally due to the concentration of Hg.

Gold and silver comprise the main alloy constituents and their concentrations within all individual placer grains are shown in figure 14. Gold grains from orogenic deposits analyses show a strong Au-Ag correlation (R= .994) and essentially all plot along a binary mixing line, with only a minimal number of grains plotting slightly away from the line. Many of the grains from alkalic porphyry-associated placers also plot along the Au-Ag correlation line, but many do not. Deviation may be caused either by co- ablation of inclusions (e.g. elevated signals of Fe and or Cu) or by other elements contributing more substantially to the alloy composition (e.g. Hg). The deviation away from

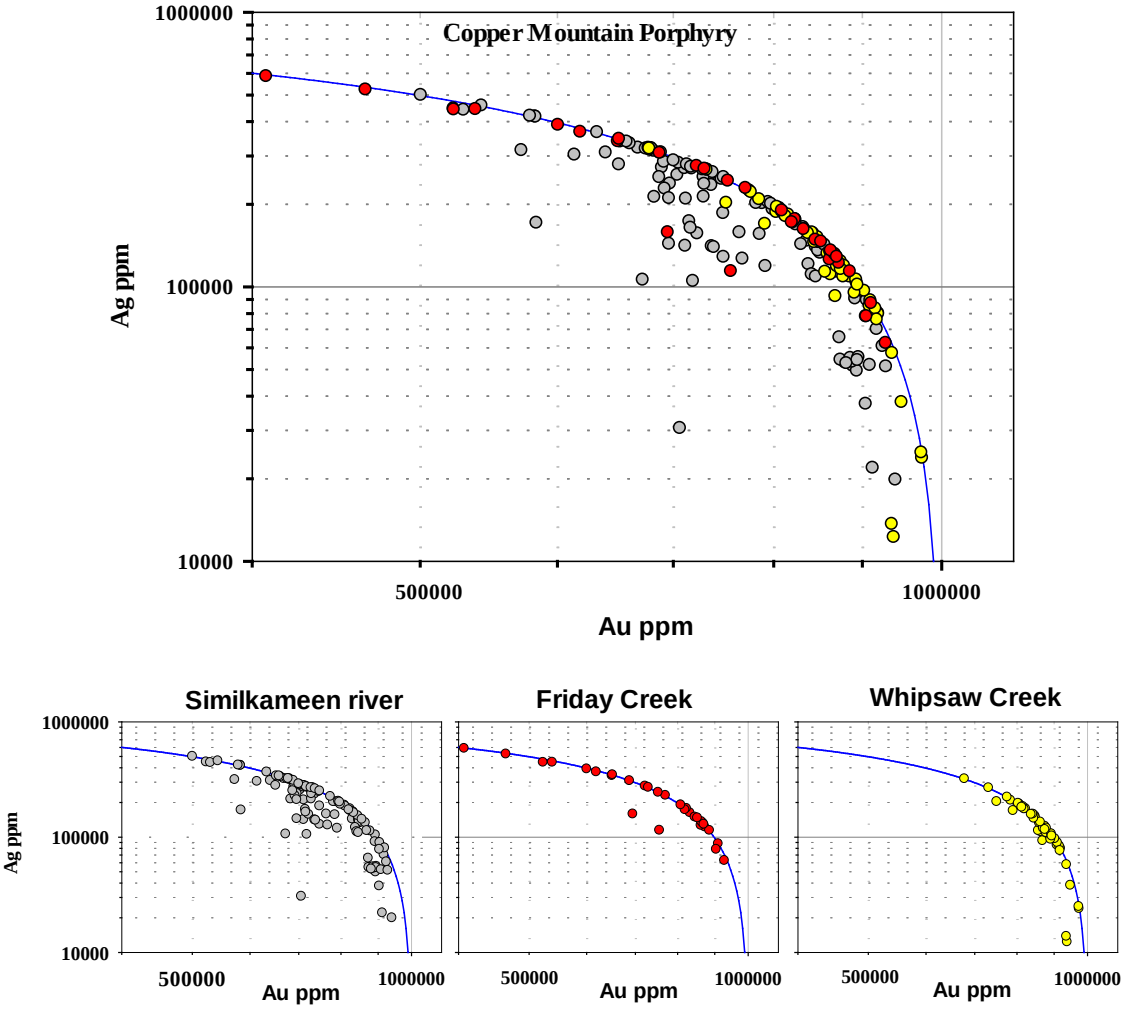

Figure 15. Au-Ag concentrations of the grains from three different drainages of the Copper Mountain porphyry. The grains from the Similkameen River have the highest Hg concentrations.

the correlation line is due to a reduction of the Ag concentration (analyses are plotting to the left) matched primarily by the increase in the Hg concentration as there is a negative correlation of Ag and Hg (bivariate plots of Ag-Hg for all the individual placers analysed are shown in the supplementary figures). This approach can be applied to a population of grains to evaluate whether there is a contribution from gold derived from an alkalic porphyry system.

The binary Au-Ag plot for all grains from the Copper Mountain area (111 grains from the Similkameen River, 46 from Whipsaw Creek and 54 from Friday Creek) is presented in figure 15. Approximately 40% of the grains analysed from the Similkameen River plot further away from the correlation defied by the grains from orogenic related deposits and therefore could be identified as originating from an alkalic porphyry source. Gold from Friday and Whipsaw creeks shows a lower degree of deviation with around 10% of each population plotting below the Au-Ag binary curve.

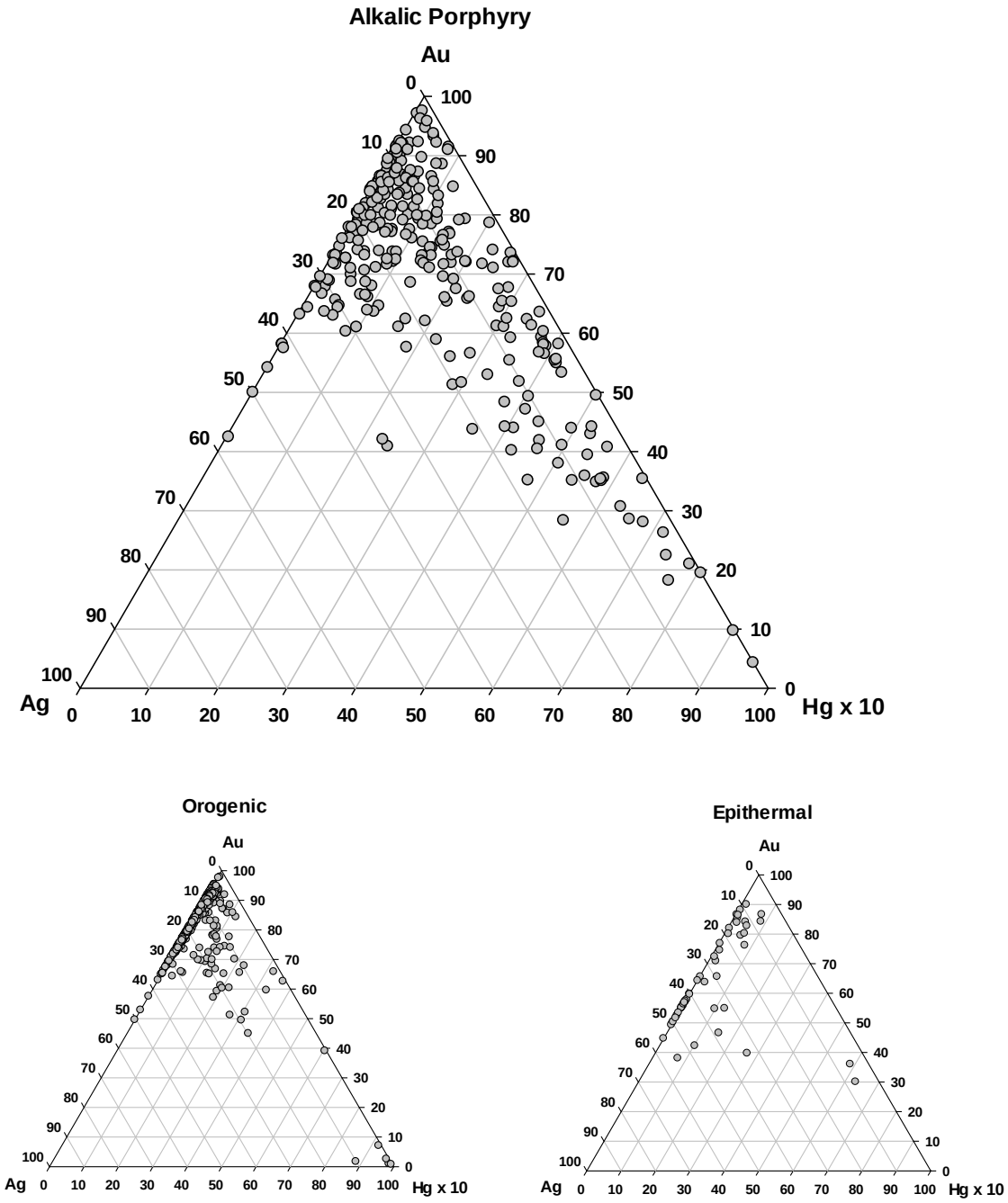

Figure 16. Relationship between Au-Ag-Hg in grains from placers with different source affinities. Mercury concentrations are highest in gold from alkalic porphyry systems.

Nevertheless this figure is still in excess of the 3% deviation recorded in the populations of orogenic gold grains. The reasons for the compositional differences in gold from Friday and Whipsaw creeks with respect to the gold from the Similkameen River is possibly related to their positions within the porphyry system. Whipsaw and Friday creeks drain the periphery of the porphyry whereas the Similkameen River dissects the central porphyry. The Copper Mountain porphyry system is complex and several gold bearing stages of mineralization have been identified, including bornite-

temagamite bearing veins in Friday Creek (see discussion in Chapman et al. 2017). In this study, Hg has proved the clearest discriminant between gold derived from orogenic and alkalic porphyry systems, although the sporadic high Pd values in au alloy previously reported by Chapman et al. (2017) are also evident.

The triangular Au-Ag-Hg plots in figure 16 emphasises the inverse relationship between Ag and Hg and that the percentage of grains from alkalic porphyry deposits with increased Hg is more than those from an orogenic source. The epithermal sourced grains have the lowest Hg values as a population, but as the data is from one placer any interpretation of this result would be speculative. However, unless an unknown population of gold grains has Hg concentrations greater than 3% it is unlikely they would have come from an alkalic porphyry source.

Townley et al. (2003) employed Au-Ag-Cu(x100) triangular plots to distinguish gold from different porphyry and epithermal sources. This approach has been adopted for the data sets generated in the present study (figure 17) but the signature of gold from alkalic porphyries does not correspond to that previously reported for Au- rich porphyries. In addition this method of presentation does not illustrate a major difference in the Cu content of gold from alkalic porphyry or orogenic sources, although more gold grains from magmatic hydrothermal systems contain Cu in the 500- 1000 ppm range. The ranges of composition of different elements within the Au alloy from all the grains is shown in figure 18, and indicates why Hg is the key discriminating element. The other elements have essentially the same range of values, but the majority of Hg analyses from alkalic or orogenic sources do not overlap, with Hg having greater concentrations in gold grains from alkalic porphyries.

Other elements analysed in the grains are most likely present in inclusions (the majority are pyrite) and figure 9 shows that the median values for Ti, Pd, Cd, In, Hg, Bi are higher in gold from alkalic porphyry deposits. Also, the average values of most of the elements in these grains are higher as are their absolute maximum values. This would reflect the greater contribution from inclusions, and and the trace elements they contain.

In conclusion it is possible to distinguish between populations of gold grains derived from alkalic porphyry deposits and orogenic hydrothermal systems by considering the deviation from a simple binary Au-Ag alloy, the concentration of Hg in the alloy, elements recorded in the bulk analyses of the gold grains and the concentration of trace elements in pyrite inclusions.

Comparison of LA-ICP-MS methodologies

The elemental mapping of gold grains by LA-ICP-MS (ToF) has provided unique information on elements present in gold grains and their distribution. The sensitivity of the mass spectrometer has revealed the element associations in the different inclusions, which are in many cases too small to observe by SEM. Over 30 elements have been identified in the gold grains either as definable mineral

species or as traces within in larger inclusions of pyrite, chalcopyrite or galena. These data have been presented as intensities as calculating actual concentrations is not trivial.

This new data set has indicated the chemical complexity of the ore fluid. Future studies would establish whether these trace elements are related to the deposit style and/or if the lithology in which the original hypogene veins were deposited was also a contributing factor to trace element distribution through fluid- rock interaction. Trace element assemblages, in conjunction with their concentrations may ultimately provide a reliable guide to gold provenance.

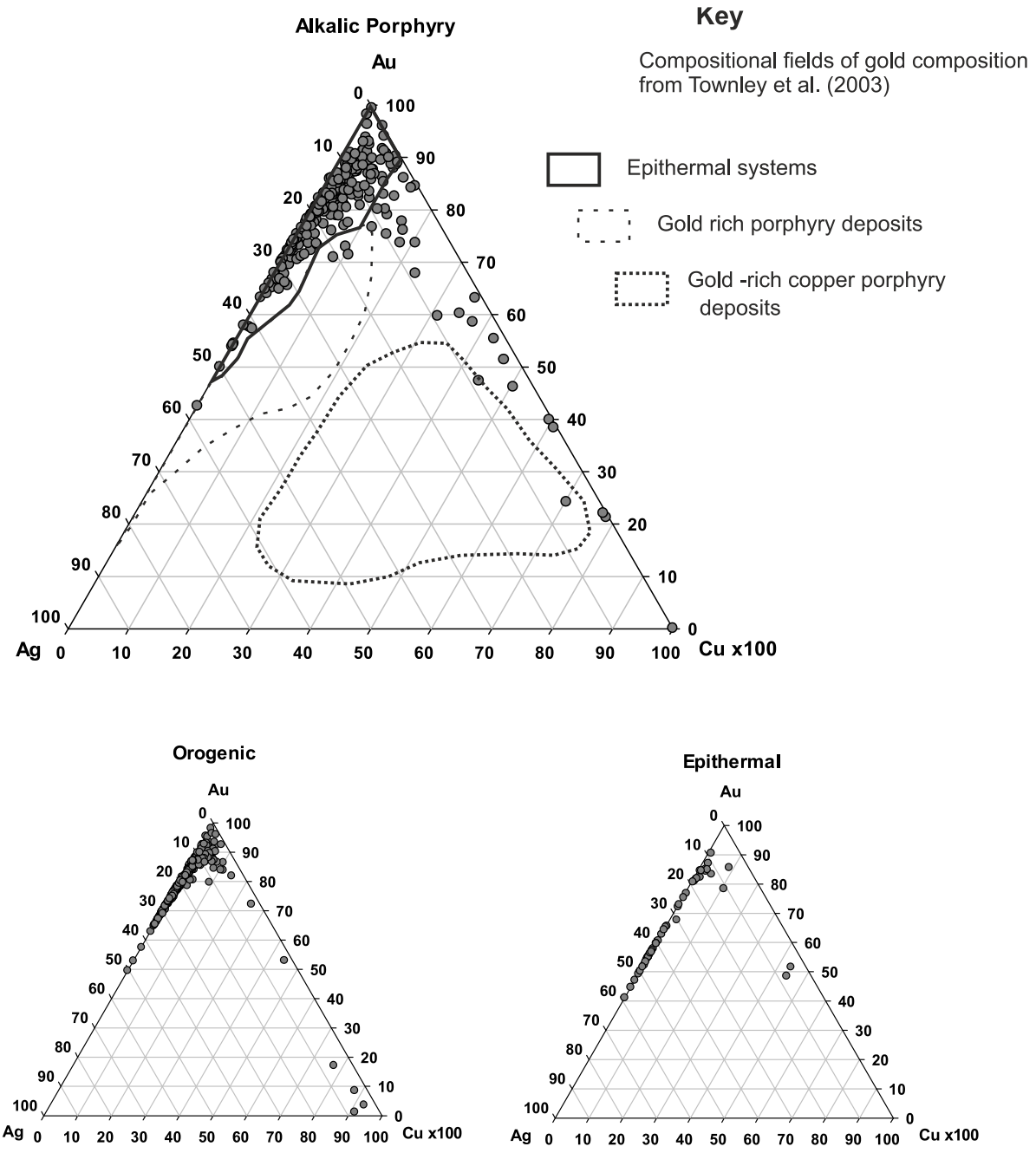

Figure 17. Au-Ag-Cu relationship of grains from the different sources. Compositional field proposed by Townley et al. (2003) shown on the main diagram.

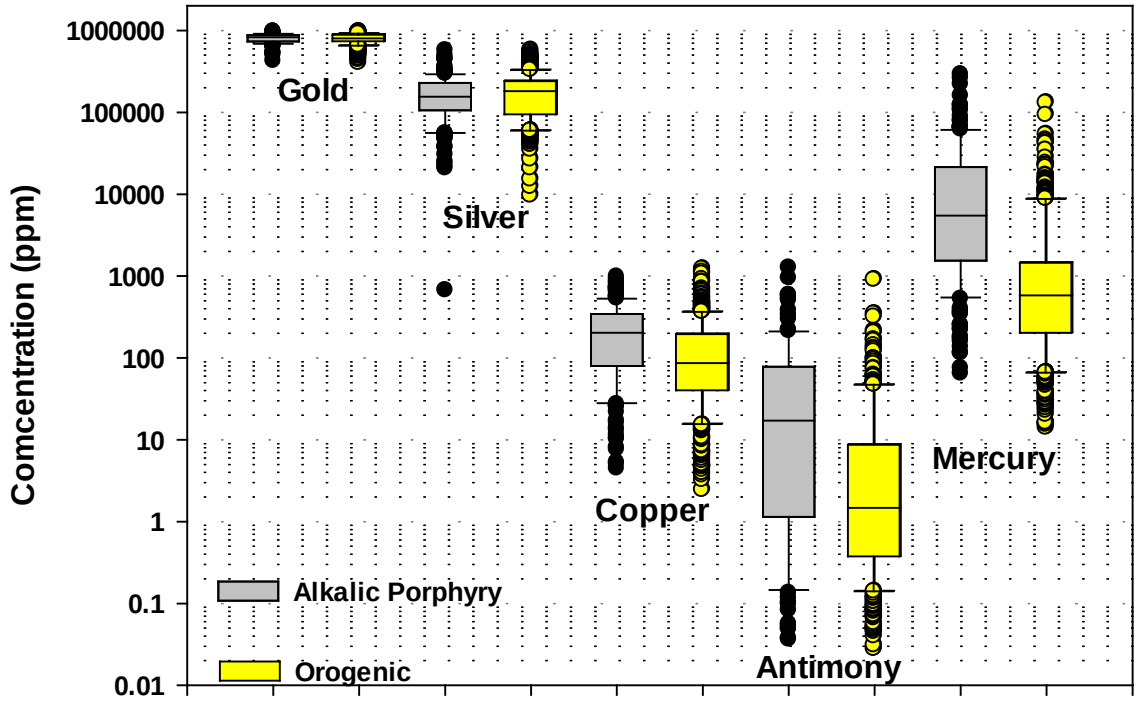

Figure 18. The range of major alloying elements present in gold derived from alkalic porphyry and orogenic systems. Mercury provides the only elemental discriminant.

Comparison of LA-ICP-MS analysis methodologies with previous work.

Chapman et al. (2017) utilised applied microchemical characterization to the same sample suites which formed the basis for the present study. This approach utilized both alloy compositions derived from EMP, and the systematic recording of micro inclusions (lower observational limit c 1µm) to characterize populations of grains according to alloy and mineralogical criteria. These authors showed that the consistently high Hg values in Au alloy coupled with sporadic but repeatable Pd values, and a Pd-Hg signature in the inclusion suite, distinguished gold from alkalic porphyries from that from other sources. The disadvantages of this approach were both that a large number of gold grains were required, and also the concentrations of Cu and Pd often spanned the LOD, such that much quantitative data was incapable of underpinning rigorous interpretation.

The adoption of LA-ICP-MS has greatly improved our ability to characterise gold alloy according to minor alloying elements. However, this project has highlighted hitherto unrecognised textural characteristics of trace element distribution within natural gold, which greatly influence the way in which data sets can be interpreted. It appears that only a small number of elements form homogeneous alloys with Au, and most exhibit localized concentrations either with the Au alloy or as inclusions too small to detect visually by SEM. Thus interpretation of the data sets must be made with caution given that this heterogeneity would have a large impact on the analytical result depending upon the site of ablation. In summary, the assumption that the adoption of LA-ICP-MS would generate larger elemental suites for use as discriminants now appears to be simplistic.

Mercury has been identified as the prime discriminant by which to distinguish gold from alkalic porphyry and orogenic sources in BC. Whilst this distinction applies to the sample populations studied here, a claim for Hg as a generic discriminant must be made with caution. Various orogenic gold systems are associated with high Hg gold, e.g., the Violet occurrence, Klondike, Yukon (max 9%) (Chapman et al. 2010) and various localities in the British Caledonides, e.g. Cavanacaw Mine, N Ireland (max 10% Hg), and Calliacher Burn, central Scottish Highlands (max 6% Hg) (Chapman et al. 2000).

The results of this study are compatible with those derived by microchemical characterization, but populations of gold grains would still be required to establish the compositional range of detrital gold to confidently speculate on the source mineralization. Currently, microchemical characterization offers the advantage of direct mineralogical characterization of inclusion assemblages, as the Pd-Hg bearing suite is diagnostic for gold from alkalic porphyry systems. Nevertheless the present study has identified new directions which could take advantage of alloy heterogeneity and the extreme partitioning of various elements to specific mineral inclusions. These new avenues of investigation will form the subject of future studies.

Conclusions

LA-ICP-MS using the quadrupole system generates analyses that are compatible with data obtained for the alloying elements commonly measurable by EMP (Au, Ag, Cu, Hg). The much lower detection limit of the LA systems has allowed many other elements in the grains to be determined, often down to ppb levels. Multi element maps generated by ToF LA-ICP-MS show element distribution within gold grains at the trace level and have revealed the complex heterogeneous nature of natural gold. Small inclusions, (smaller than may be observed using the SEM) appear generally common, but their characterization depends on both their presence within the column of ablated material and the detection of all their component elements during the elemental scans by the quadrupole system. In contrast, the multi element maps generated by the ToF-MS clearly identify the association of the different elements. Both approaches have demonstrated that the degree of heterogeneity of the same element within gold grains may differ substantially between grains from the same sampling locality.

Analyses of the alloy composition of grains from both alkalic porphyry and orogenic environments generated similar ranges of Au-Ag-Cu-Sb concentrations within gold. Individual irregularities have been ascribed to ablation of inclusions, which appear to be more common in gold from magmatic hydrothermal systems. In general, the signature of gold from the alkalic porphyry systems is both more complex (indicating a corresponding complexity in the ore fluid) and richer in minor components (indicating higher concentrations of metals in solution).

Mercury provides the main discriminant by which gold from alkalic porphyry systems and orogenic systems may be differentiated using LA-ICP-MS. However Hg is present to equivalent levels in gold from some orogenic gold systems globally, whereas the Pd-Hg- bearing mineral inclusions identified using the methodology of microchemical characterization are diagnostic for gold derived from alkalic porphyry systems.

At present, the adoption of LA-ICP-MS has not reduced the number of gold grains required to confidently establish the source mineralization. This result was not expected but is a consequence of the heterogeneity of natural gold at trace element level, which has been identified here for the first time. However the study has shown that common inclusions within gold such as pyrite act as trace element sinks, and that this signature varies according to source style of mineralization. In conclusion, whilst the project has not alleviated a practical aspect of using gold as an indicator mineral through reduction of the sample size required, it has opened up various possibilities for future study which could be capable of underpinning more sophisticated approaches.

References

Antweiler, J.C. and Campbell, W.L. (1977): Application of gold compositional analyses to mineral exploration in the United States; Journal of Exploration Geochemistry, v. 8, p. 17–29.

Bouzari, F., Hart, C.J.R., Barker, S. and Bissig, T. (2010). Porphyry indicator minerals (PIMs): exploration for concealed deposits in south central British Columbia (NTS 092I/06, 093A/12, 093N/01, /14); *in* Geoscience BC Summary of Activities 2009, Geoscience BC, Report 2010-1, p. 25–32.

Celis, M.A., Bouzari, F., Bissig, T., Hart, C.J.R. and Ferbey, T, (2014). Petrographic characteristics of porphyry indicator minerals from alkalic porphyry copper-gold deposits in south-central British Columbia (NTS 092, 093); *in* Geoscience BC Summary of Activities 2013, Geoscience BC, Report 2014-1, p. 53–62.

Chapman RJ, Leake RC, Moles NR, Earls G, Cooper C, Harrington K, Berzins R. 2000. The application of microchemical analysis of alluvial gold grains to the understanding of complex local and regional gold mineralization: A case study in the Irish and Scottish caledonides. Economic Geology . 95(8), pp. 1753-1773.

Chapman RJ, Leake RC, Bond DPG, Stedra V, Fairgrieve B. 2009. Chemical and Mineralogical Signatures of Gold Formed in Oxidizing Chloride Hydrothermal Systems and their Significance within Populations of Placer Gold Grains Collected during Reconnaissance. Economic Geology 104(4), pp. 563-585.

Chapman RJ, Mortensen JK, LeBarge WL, Crawford EC. 2010. Microchemical Studies of Placer and Lode Gold in the Klondike District, Yukon, Canada: 2. Constraints on the Nature and Location of Regional Lode Sources. Economic Geology. 105, pp. 1393-1410.

Chapman RJ, Mortensen JK, LeBarge WL, Crawford EC. 2010. Microchemical Studies of Placer and Lode Gold in the Klondike District, Yukon, Canada: 1. Evidence for a Small, Gold-Rich, Orogenic Hydrothermal System in the Bonanza and Eldorado Creek Area. Economic Geology. 105, pp. 1369-1392.

Chapman RJ, Mortensen JK. 2016. Characterization of gold mineralization in the northern Cariboo gold district, British Columbia, Canada, through integration of compositional studies of lode and detrital gold with historical placer production: A template for evaluation of orogenic gold districts. Economic Geology. 111(6), pp. 1321-1345

Chapman RJ, Mileham T, Allan M, Mortensen J. 2017. A Distinctive Pd-Hg Signature in Detrital Gold Derived from Alkalic Cu-Au Porphyry Systems. Ore Geology Reviews. 83, pp. 84-102

Chapman RJ, Allan MM, Mortensen JK, Wrighton TM, Grimshaw MR. 2018. A new indicator mineral methodology based on a generic Bi-Pb-Te-S mineral inclusion signature in detrital gold from porphyry and low/intermediate sulfidation epithermal environments in Yukon Territory, Canada. Mineralium Deposita. 53(6), pp. 815-834

Guillong, M., Meier, D.L., Allam, M.M., Heinrich, C. and Yardley, B.W.D. (2008). SILLS a MATLAB-based program for the reduction of laser ablation ICP-MS data of homogeneous materials and inclusions. In.: Sylvester, P. (ed.) Laser Ablation ICP-MS in the Earth Sciences: Current Practices and Outstanding Issues. Vancouver, B.C. Mineralogical Association of Canada Short Course 40, 328-333.

Kelly, K.D., Eppinger, R.G., Lang, J., Smith, S.M and Fey, D.L. (2011). Porphyry Cu indicator minerals in till as an exploration tool: example from the giant Pebble porphyry Cu-Au-Mo deposit, Alaska, USA. Geochemistry: Exploration, Environment, Analysis, *v.* 11, p. 321-334.

Knight, J.B., Mortensen, J.K. and Morison, S.R. (1999): Lode and placer gold composition in the Klondike District, Yukon Territory, Canada: implications for the nature and genesis of Klondike placer and lode gold deposits; Economic Geology, v. 94, p. 649–664

Pisiak, L.K., Canil, D., Grondahl, C., Plouffe, A., Ferbey, T. and Anderson, R.G. (2015): Magnetite as a porphyry copper indicator mineral in till: a test using the Mount Polley porphyry copper-gold deposit, south-central British Columbia (NTS 093A); *in* Geoscience BC Summary of Activities 2014, Geoscience BC, Report 2015-1, p. 141-150.

McTaggart, K.C., and Knight, J., 1993, Geochemistry of lode and placer gold of the Cariboo District, BC: British Columbia Ministry of Energy, Mines and Petroleum Resources, Open File 1993-30, 25 p.

Mortensen, J.K., and Chapman, R., 2010, Characterization of placer- and lode-gold grains as an exploration tool in east-central British Columbia (NTS 093A, B, G, H): Geoscience BC, Report 2011-1, p. 65–76.

Plouffe, A., Ferbey, T., Anderson, R.G., Hashmi, S. and Ward, B.C.((2013): New TGI-4 till geochemistry and mineralogy results near the Highland Valley, Gibraltar, and Mount Polley mines, and Woodjam District: an aid to search for buried porphyry deposits; Geological Survey of Canada, Open File 7473, 58 p.

Potter, M., and Styles, M.T., 2003, Gold characterization as a guide to bedrock sources for the Estero Hondo alluvial gold mine, western Ecuador: Transactions of the Institution of Mining and Metallurgy (Section B Applied Earth Sciences), v. 112, p. 297–304

Townley, B.K., Herail, G., Maksaev, V., Palacios, C., de Parseval, P., Sepuldeva, F., Orellana, R., Rivas, P., and Ulloa, C., 2003, Gold grain morphology and composition as an exploration tool: Application to gold exploration in covered areas: Geochemistry, Exploration, Environment, Analysis, v. 3, p. 29–38

Supplementary Figures

The following supplementary figures are bivariate plots of the main alloy elements in the gold grains from the different sources and on a deposit by deposit basis. In the main body of the report this data was presented as box and whisker plots to show the ranges for orogenic vs alkalic porphyry. Here the distribution of analyses within each deposit can be assessed and in many shows a quite restricted range.

The box and whisker plots of Au, Ag, Cu, Sb, Hg show the concentration ranges in the gold alloy when ablation did not intersect any inclusions (alloy) and when inclusions were ablated but it was still possible to process only the gold alloy component during ablation (inclusions).

The bivariate element plots use the individual analyses obtained from the alloy of both inclusion and alloy groups.

Friday Ck.

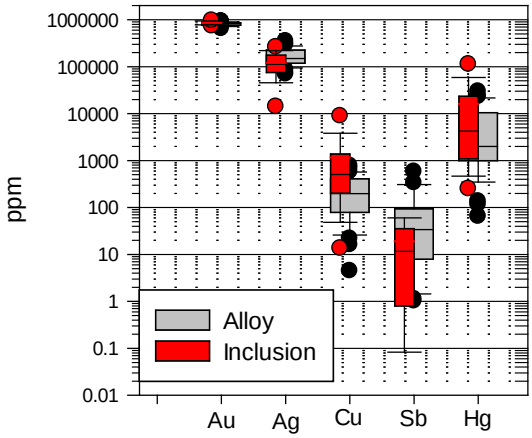

Cherry Ck.

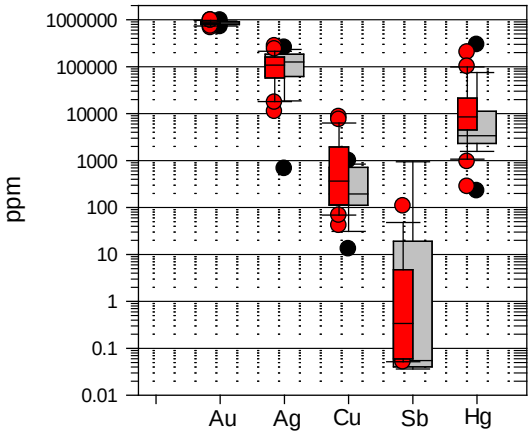

Whipsaw Ck.

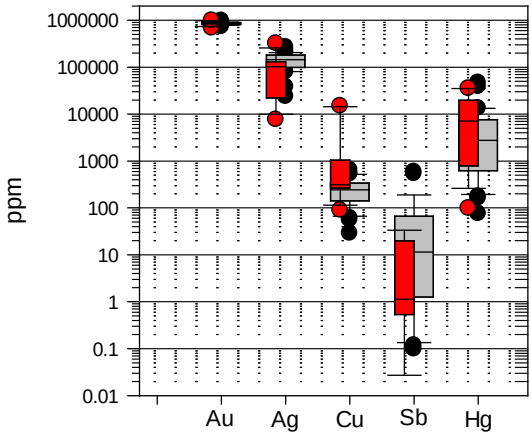

King Richard Ck.

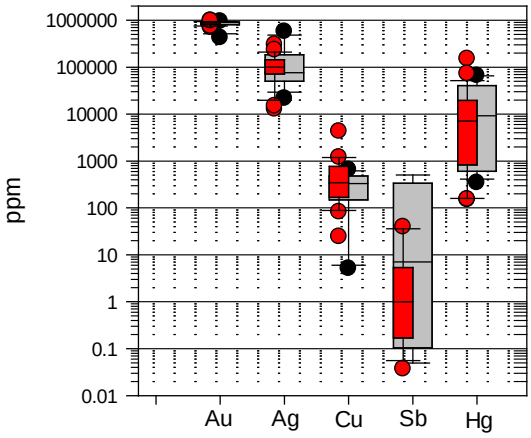

Similkameen

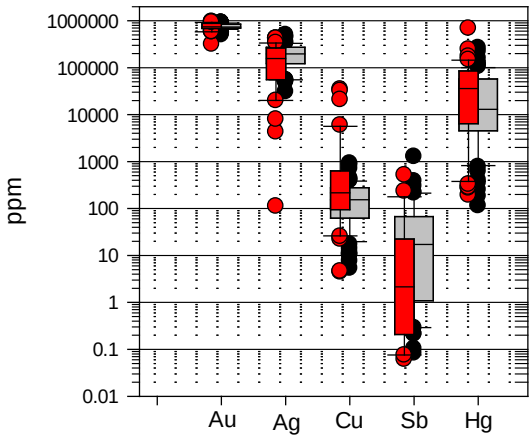

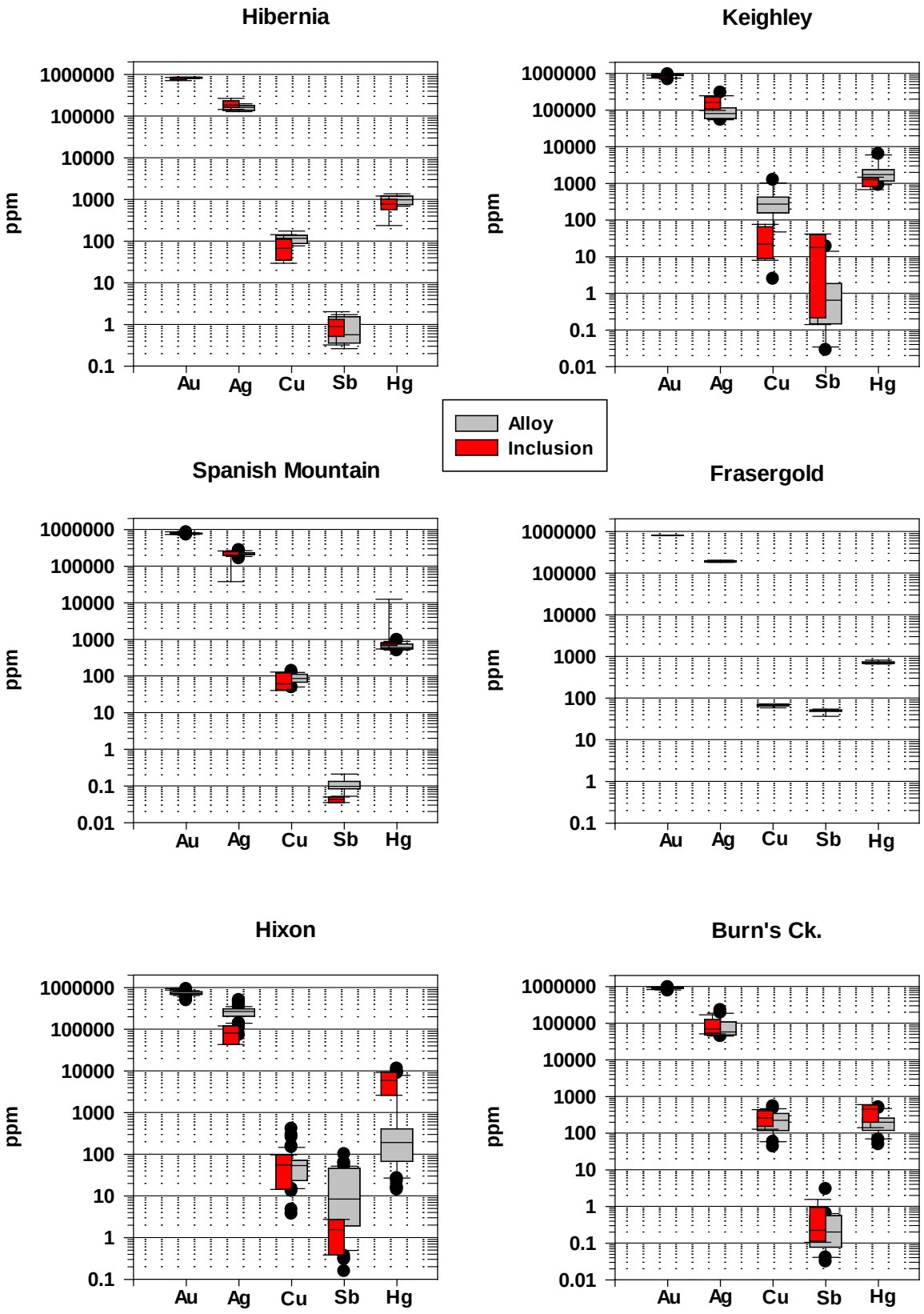
Hibernia
Keighley
Spanish Mountain
Frasergold
Hixon
Burn's Ck.
ppm
1000000
100000
10000
1000
100
10
1
0.1
0.01
Au
Ag
Cu
Sb
Hg
Alloy
Inclusion

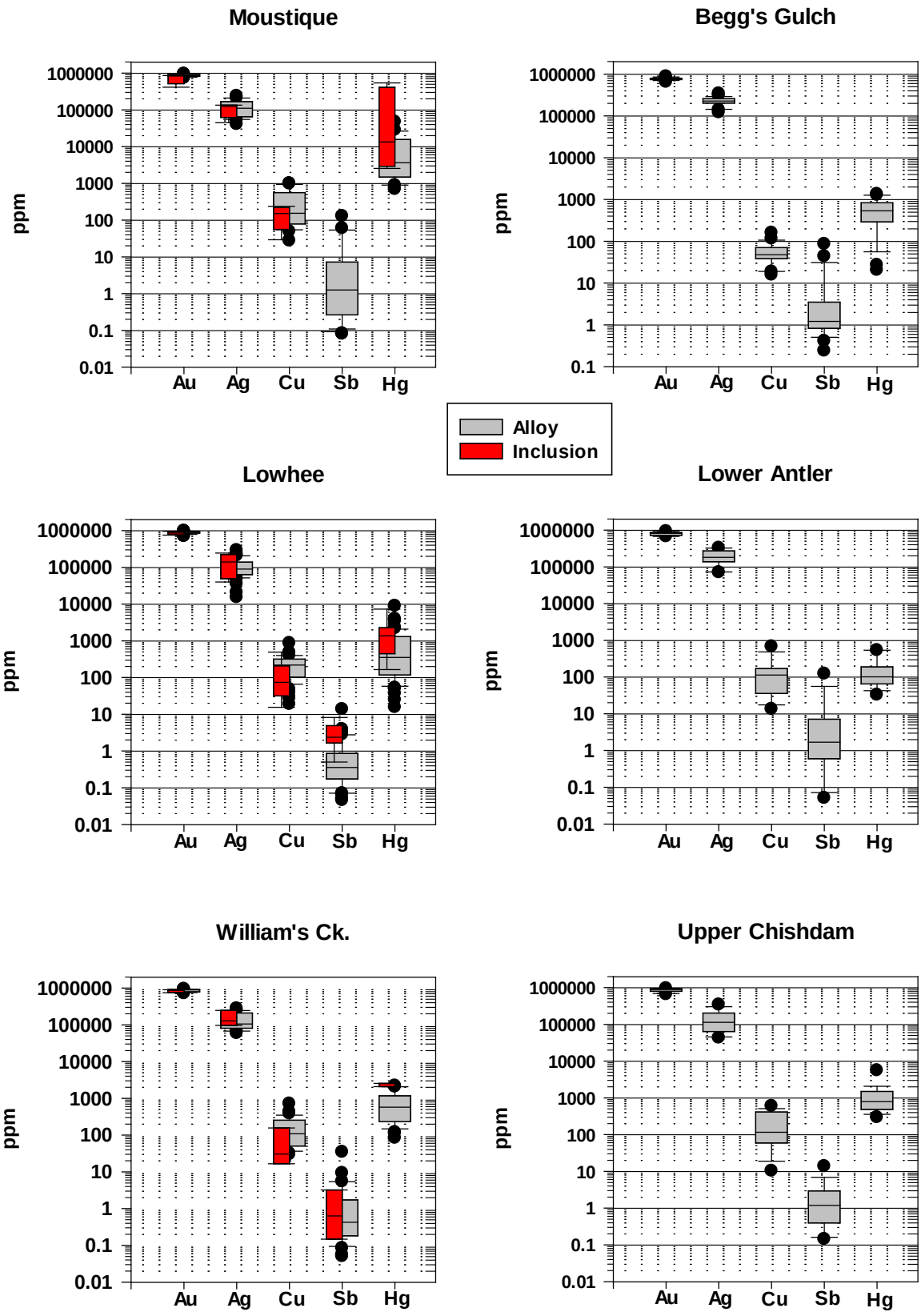
Moustique
Begg's Gulch
Lowhee
Lower Antler
William's Ck.
Upper Chishdam
ppm
1000000
100000
10000
1000
100
10
1
0.1
0.01
Au
Ag
Cu
Sb
Hg
Alloy
Inclusion

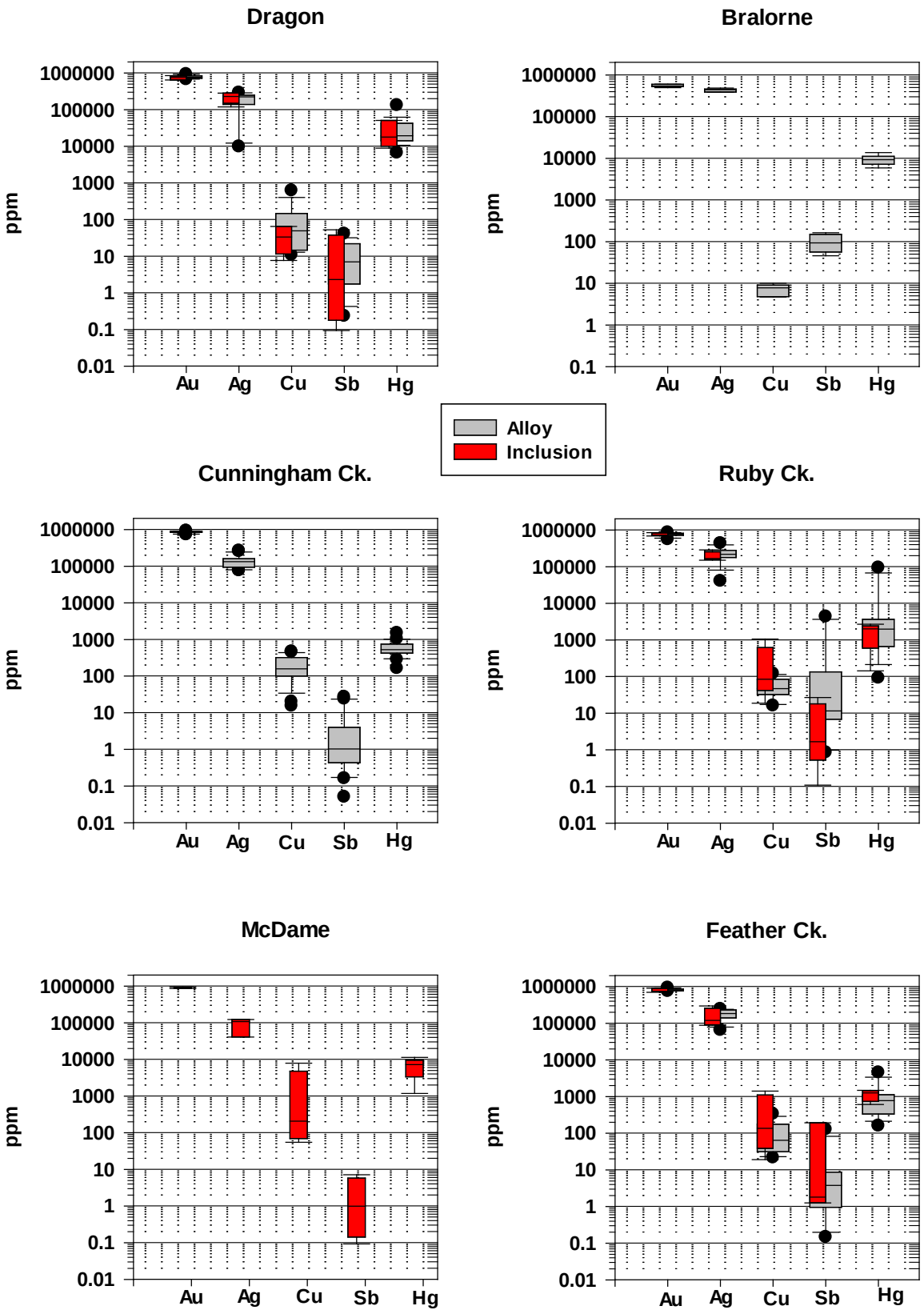
Dragon
Bralorne
Cunningham Ck.
Ruby Ck.
McDame
Feather Ck.
ppm
1000000
100000
10000
1000
100
10
1
0.1
0.01
Au
Ag
Cu
Sb
Hg
Alloy
Inclusion

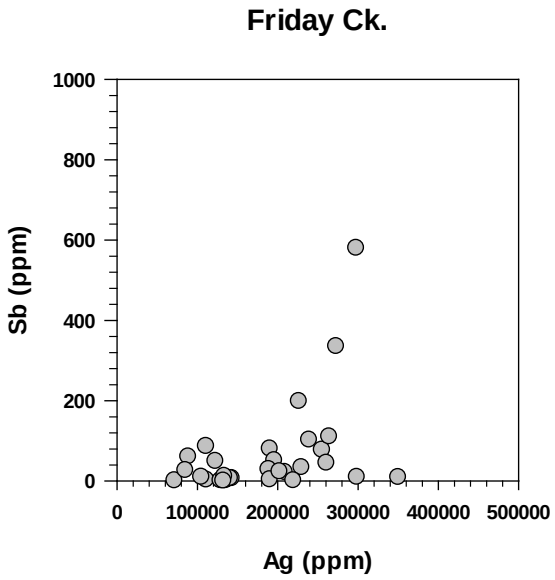
Friday Ck.
Sb (ppm)
Ag (ppm)
0
200
400
600
800
1000
0
100000
200000
300000
400000
500000

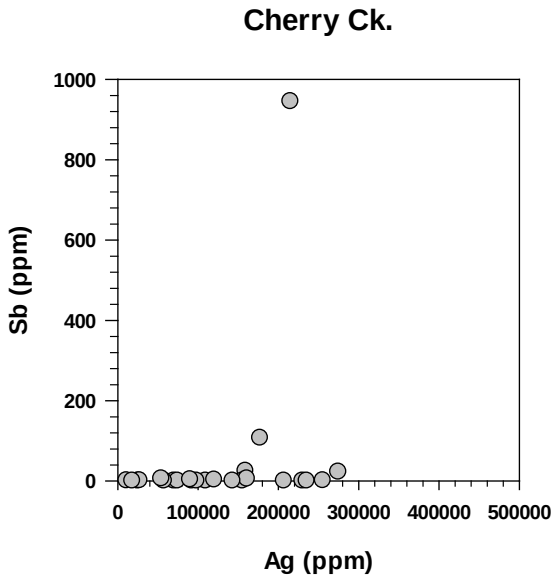
Cherry Ck.
Sb (ppm)
Ag (ppm)
0
200
400
600
800
1000
0
100000
200000
300000
400000
500000

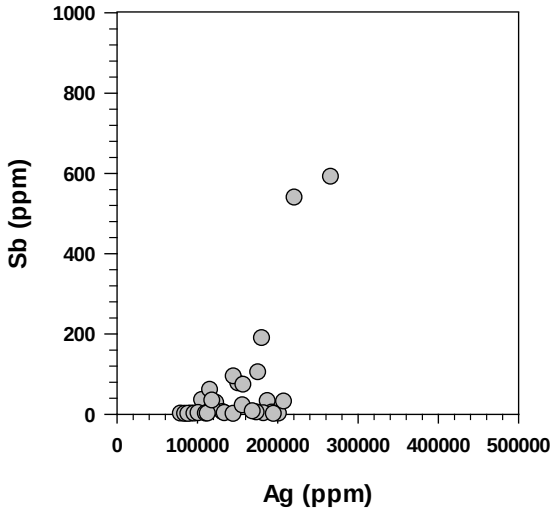
Whipsaw Ck.
Sb (ppm)
Ag (ppm)
0
200
400
600
800
1000
0
100000
200000
300000
400000
500000

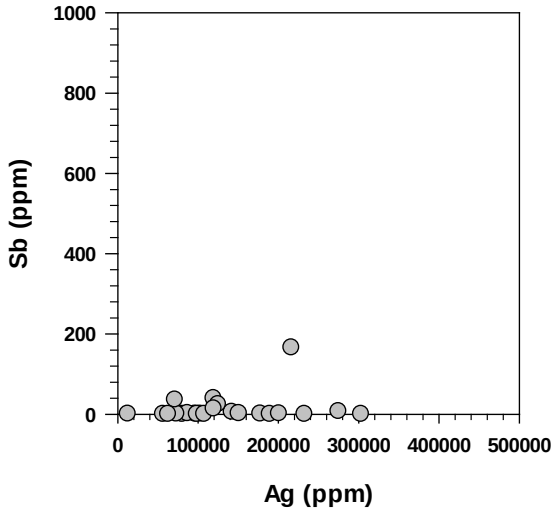
King Richard Ck.
Sb (ppm)
Ag (ppm)
0
200
400
600
800
1000
0
100000
200000
300000
400000
500000

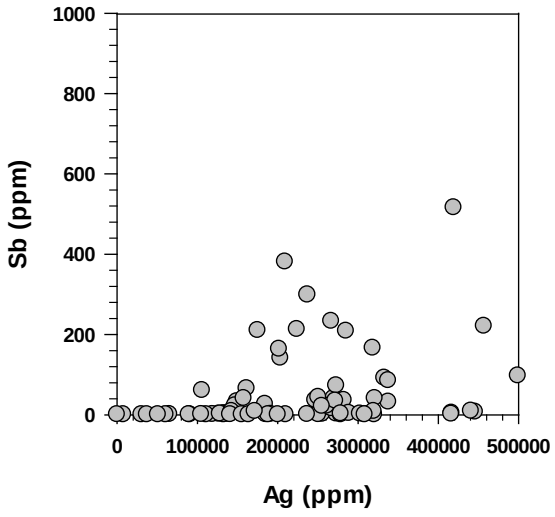
Similkameen
Sb (ppm)
Ag (ppm)
0
200
400
600
800
1000
0
100000
200000
300000
400000
500000

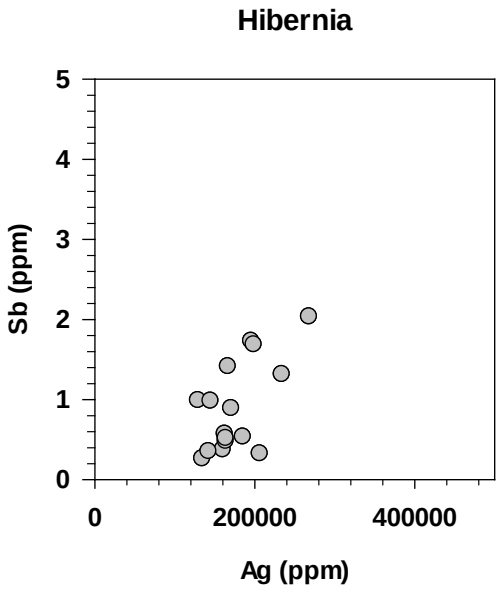
Hibernia
Sb (ppm)
Ag (ppm)
0
1
2
3
4
5
0
200000
400000

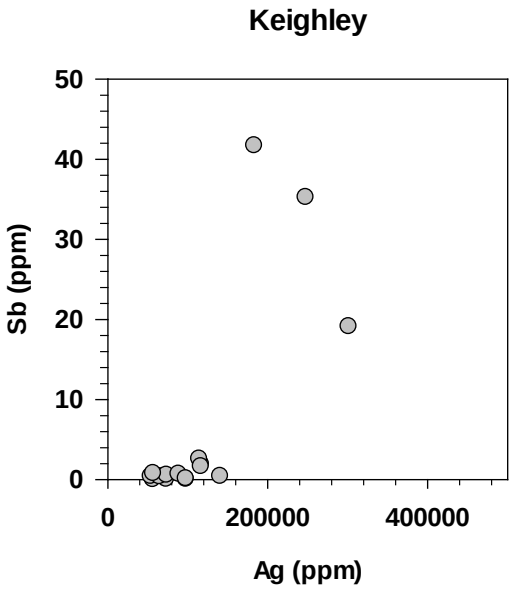
Keighley
Sb (ppm)
Ag (ppm)
0
10
20
30
40
50
0
200000
400000

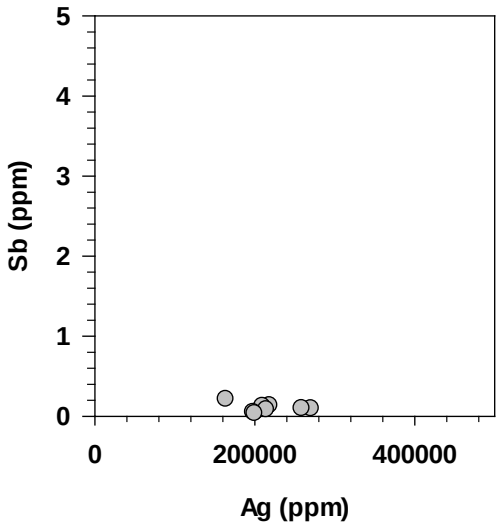
Spanish Mt.
Sb (ppm)
Ag (ppm)
0
1
2
3
4
5
0
200000
400000

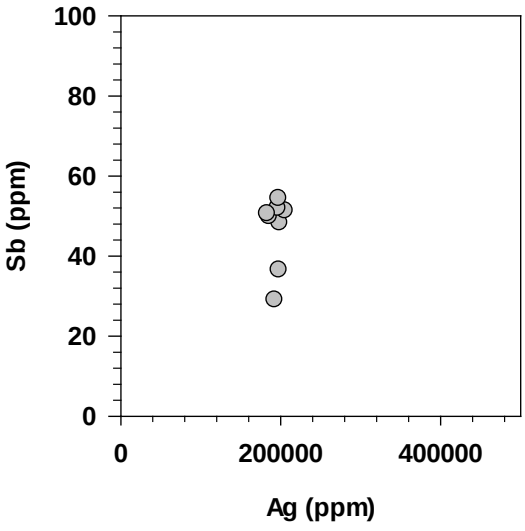
Frasergold
Sb (ppm)
Ag (ppm)
0
20
40
60
80
100
0
200000
400000

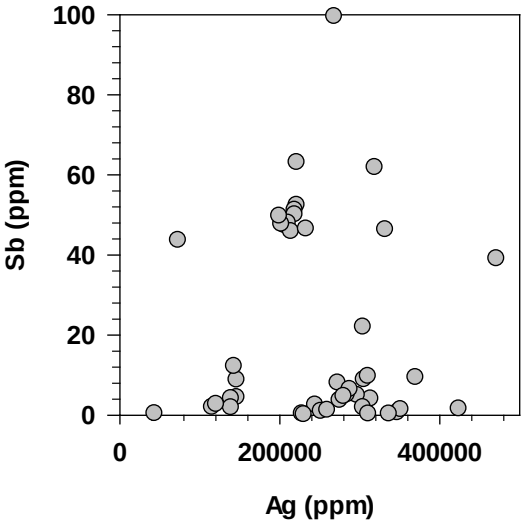
Hixon
Sb (ppm)
Ag (ppm)
0
20
40
60
80
100
0
200000
400000

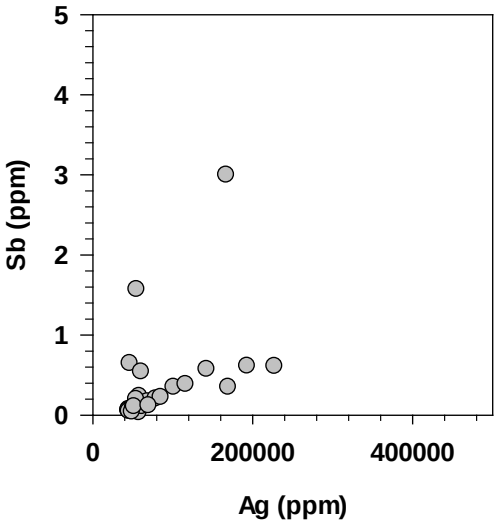
Burns Ck.
Sb (ppm)
Ag (ppm)
0
1
2
3
4
5
0
200000
400000

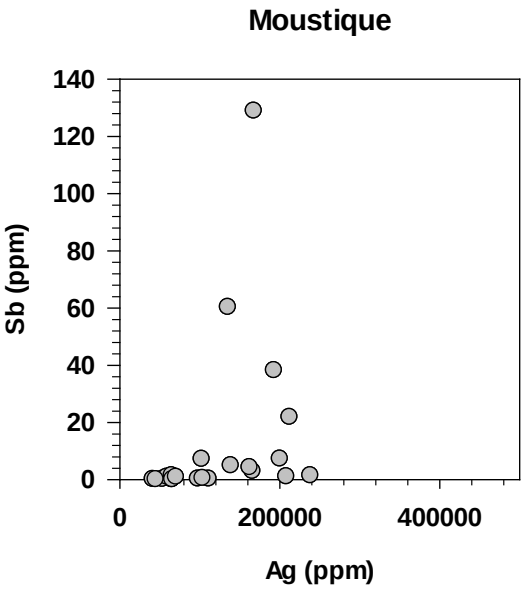
Moustique
Sb (ppm)
Ag (ppm)
0
20
40
60
80
100
120
140
0
200000
400000

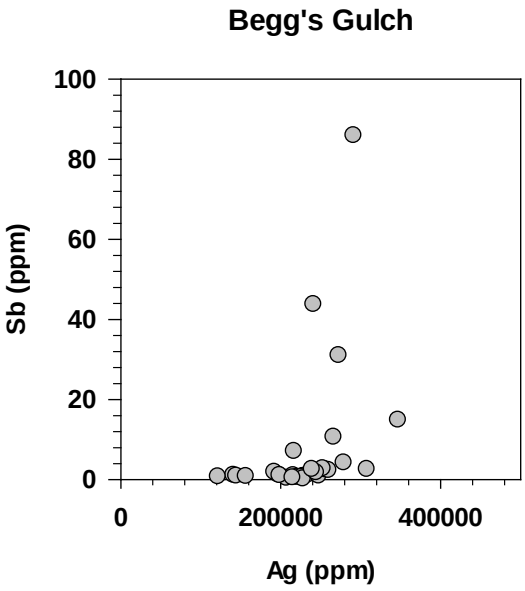
Begg's Gulch
Sb (ppm)
Ag (ppm)
0
20
40
60
80
100
0
200000
400000

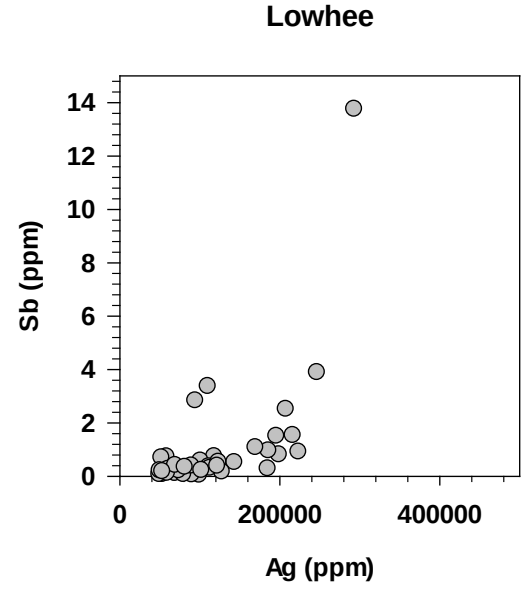
Lowhee
Sb (ppm)
Ag (ppm)
0
2
4
6
8
10
12
14
0
200000
400000

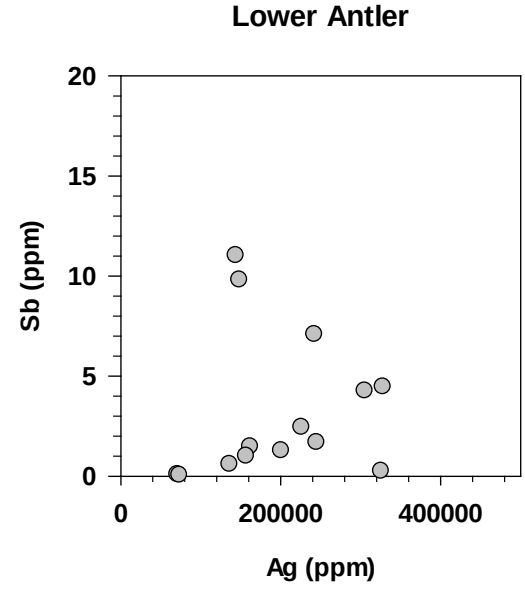
Lower Antler
Sb (ppm)
Ag (ppm)
0
5
10
15
20
0
200000
400000

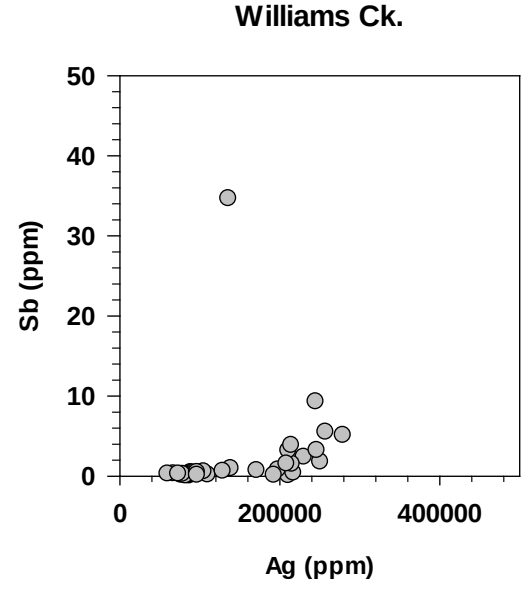
Williams Ck.
Sb (ppm)
Ag (ppm)
0
10
20
30
40
50
0
200000
400000

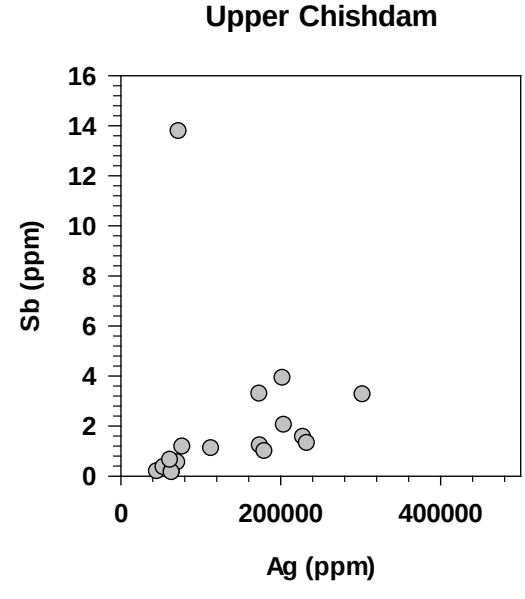
Upper Chishdam
Sb (ppm)
Ag (ppm)
0
2
4
6
8
10
12
14
16
0
200000
400000

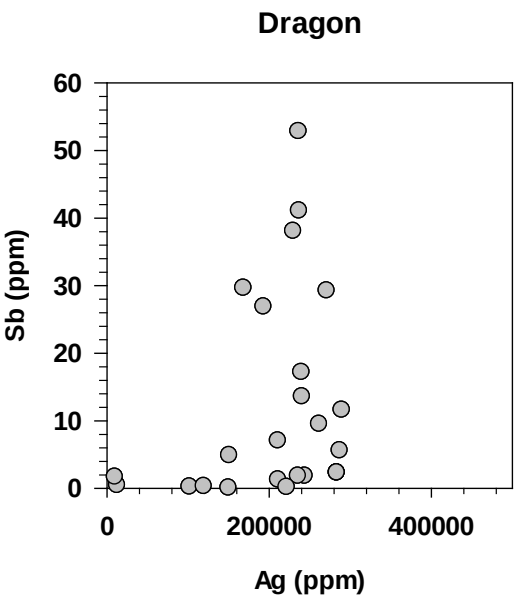
Dragon
Sb (ppm)
Ag (ppm)
0
10
20
30
40
50
60
0
200000
400000

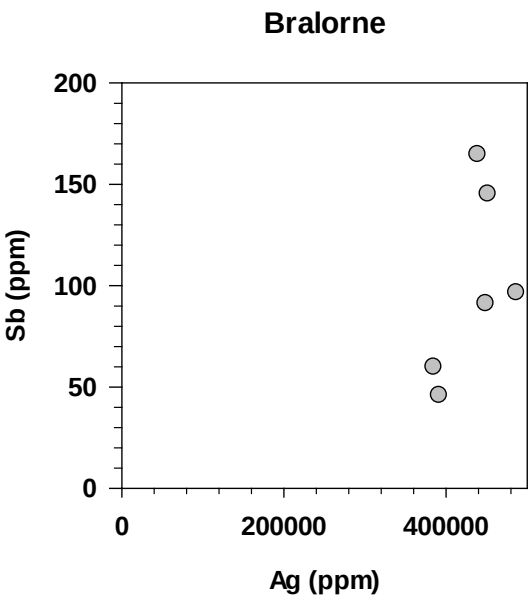
Bralorne
Sb (ppm)
Ag (ppm)
0
50
100
150
200
0
200000
400000

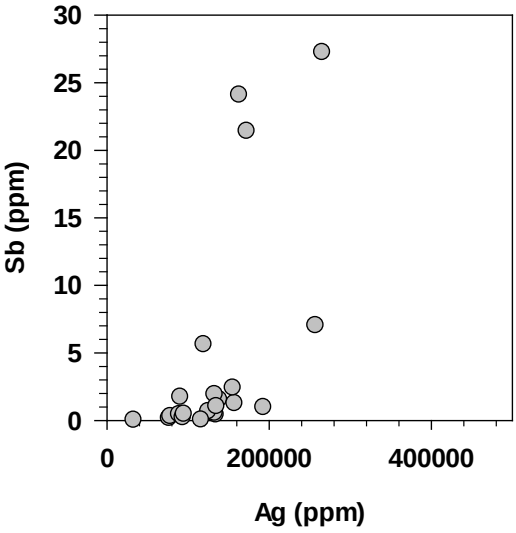
Cunningham Ck.
Sb (ppm)
Ag (ppm)
0
5
10
15
20
25
30
0
200000
400000

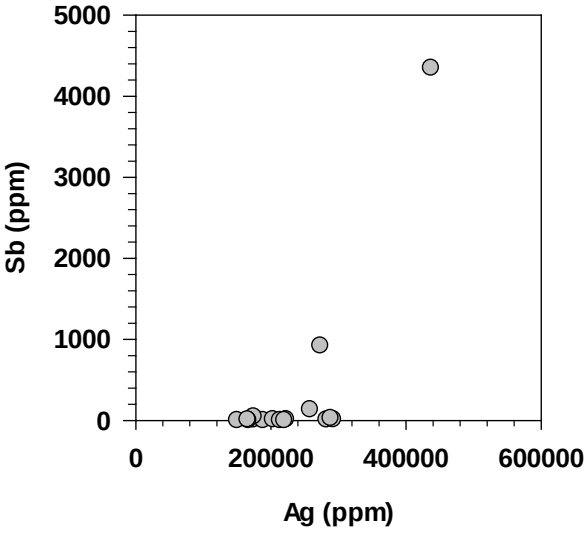
Ruby Ck.
Sb (ppm)
Ag (ppm)
0
1000
2000
3000
4000
5000
0
200000
400000
600000

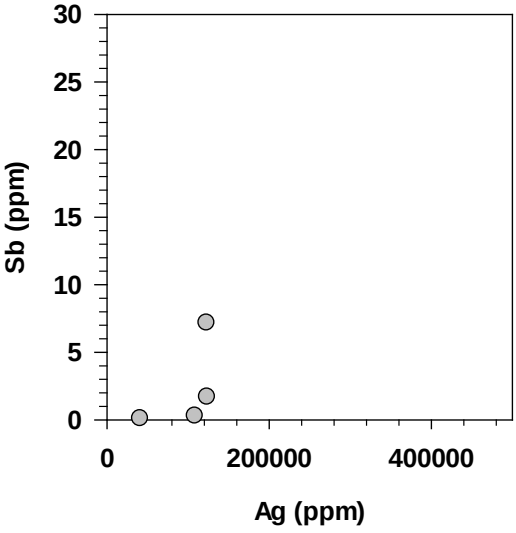
McDame
Sb (ppm)
Ag (ppm)
0
5
10
15
20
25
30
0
200000
400000

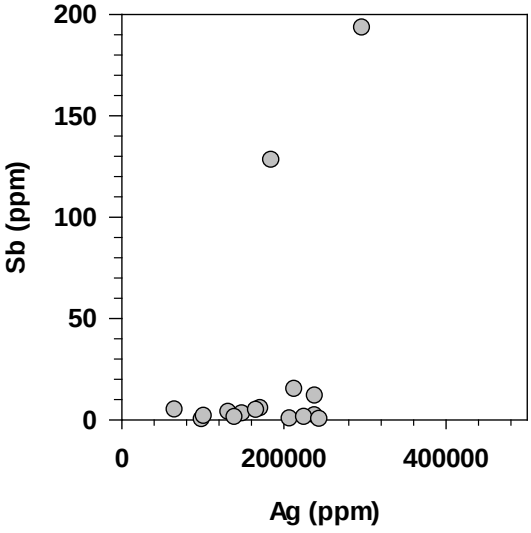
Feather Ck.
Sb (ppm)
Ag (ppm)
0
50
100
150
200
0
200000
400000

Friday Ck.

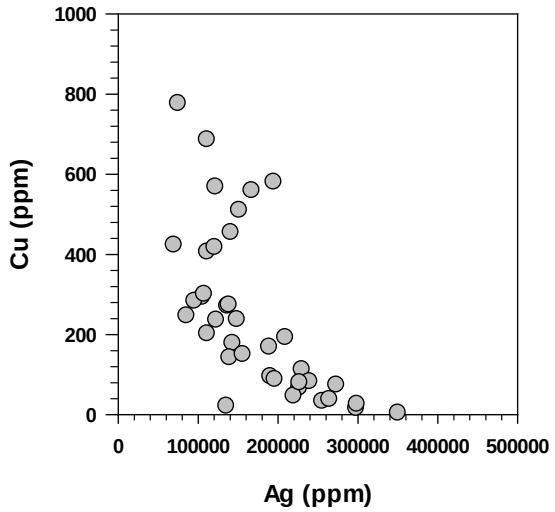

Cherry Ck.

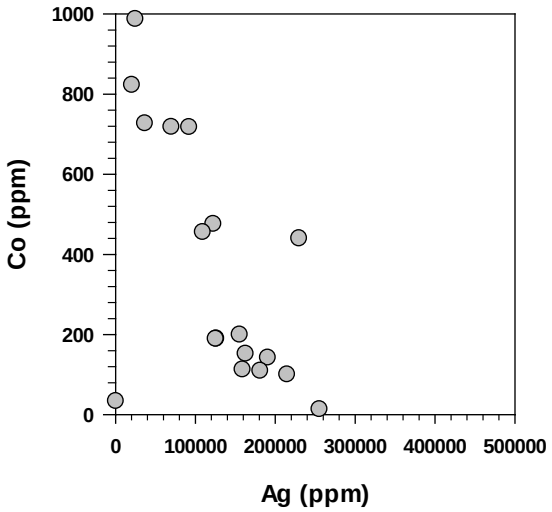

Whipsaw Ck.

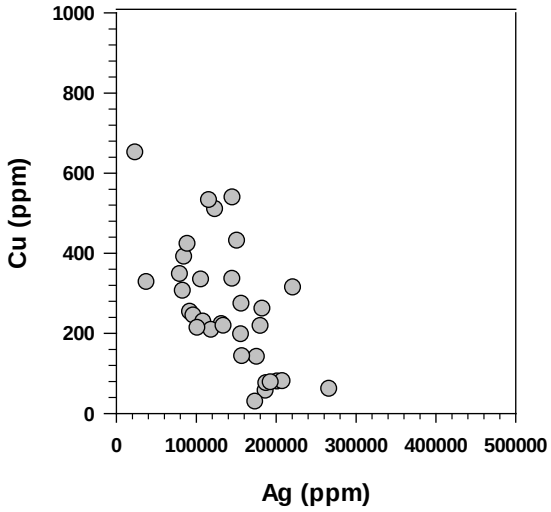

King Richard Ck.

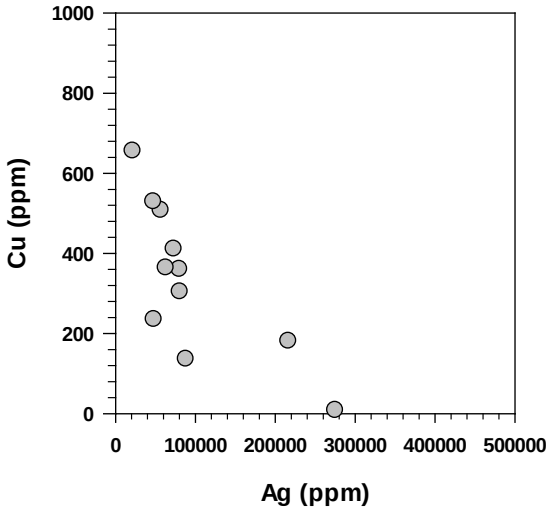

Similkameen

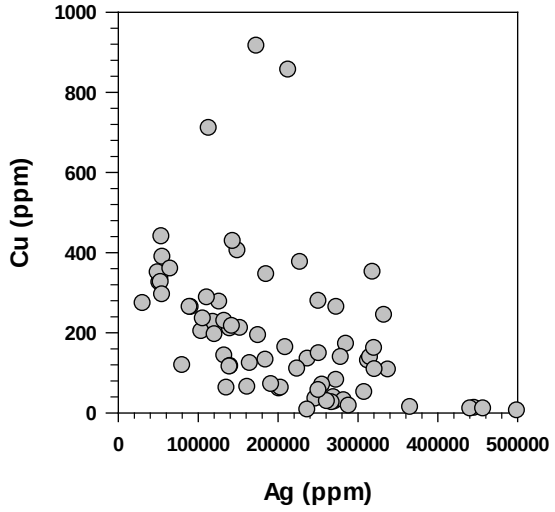

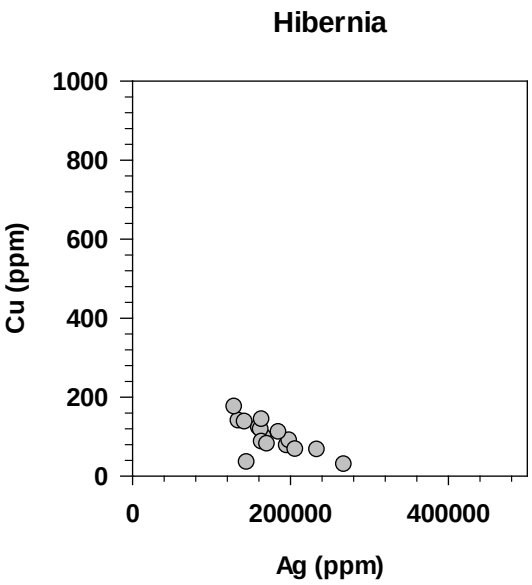
Hibernia
Cu (ppm)
1000
800
600
400
200
0
0
200000
400000
Ag (ppm)

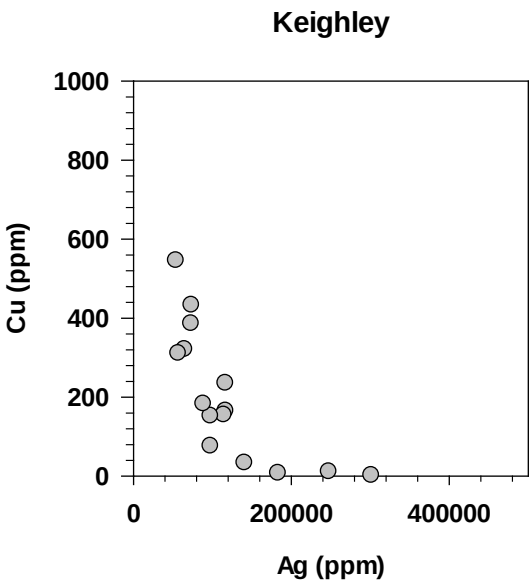
Keighley
Cu (ppm)
1000
800
600
400
200
0
0
200000
400000
Ag (ppm)

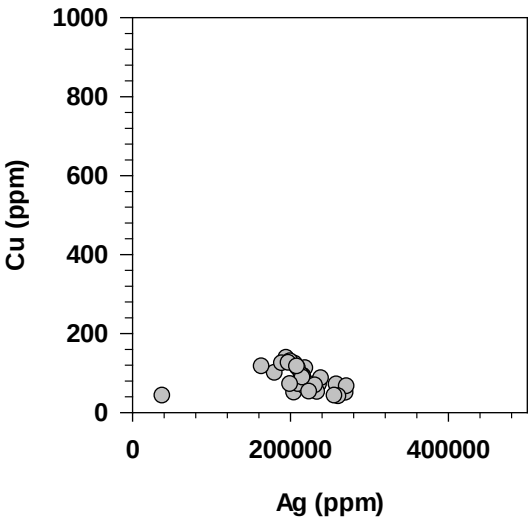
Spanish Mt.
Cu (ppm)
1000
800
600
400
200
0
0
200000
400000
Ag (ppm)

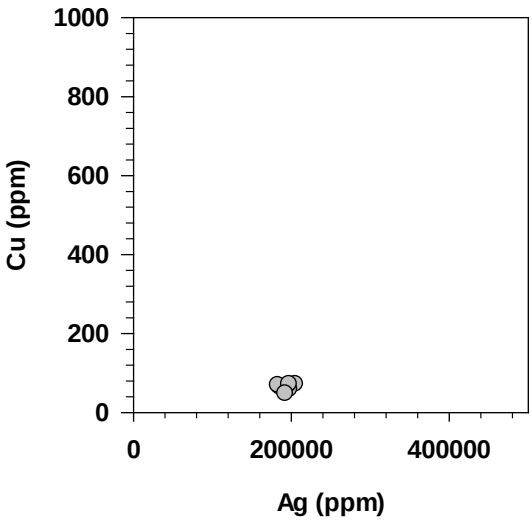
Frasergold
Cu (ppm)
1000
800
600
400
200
0
0
200000
400000
Ag (ppm)

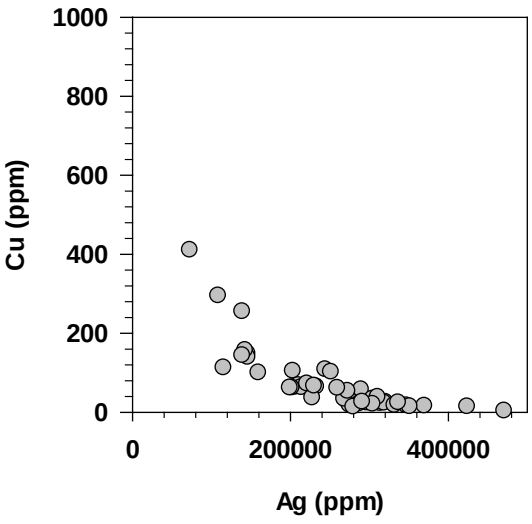
Hixon
Cu (ppm)
1000
800
600
400
200
0
0
200000
400000
Ag (ppm)

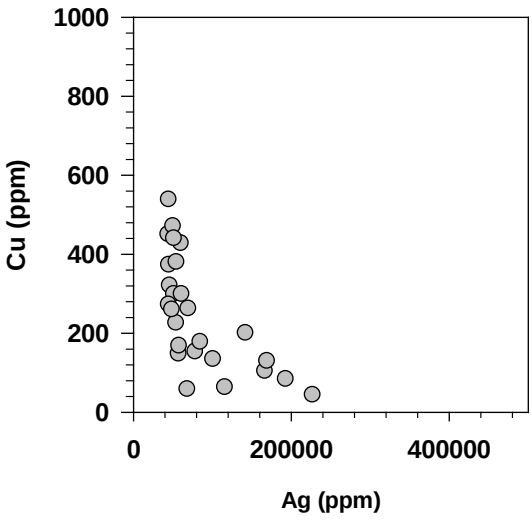
Burns Ck.
Cu (ppm)
1000
800
600
400
200
0
0
200000
400000
Ag (ppm)

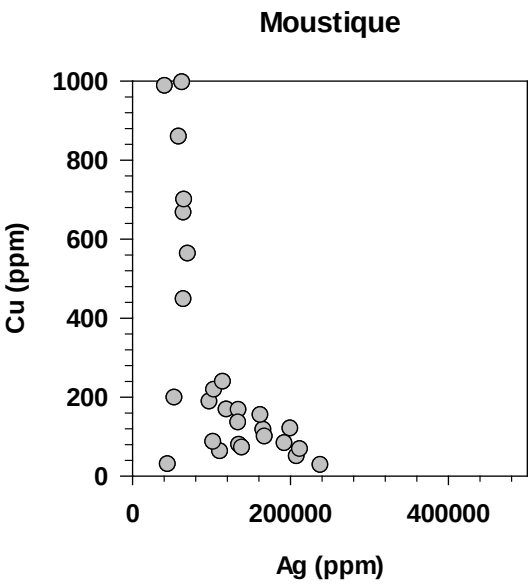
Moustique
Cu (ppm)
1000
800
600
400
200
0
0
200000
400000
Ag (ppm)

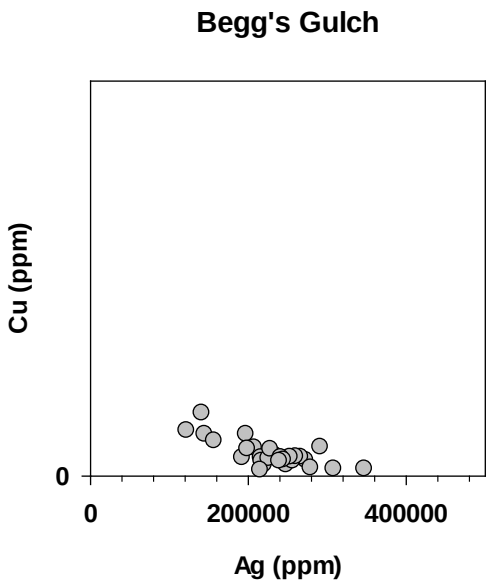
Begg's Gulch
Cu (ppm)
0
0
200000
400000
Ag (ppm)

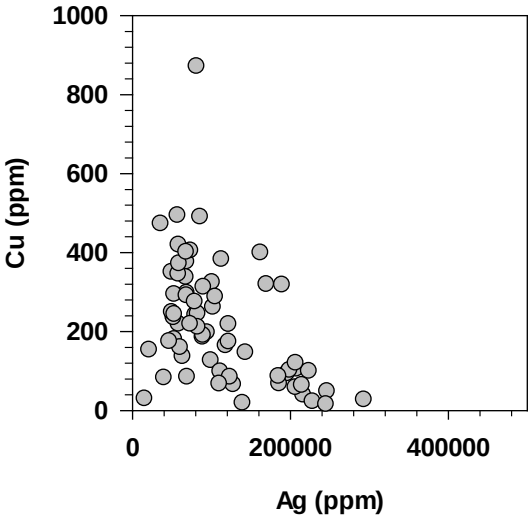
Lowhee
Cu (ppm)
1000
800
600
400
200
0
0
200000
400000
Ag (ppm)

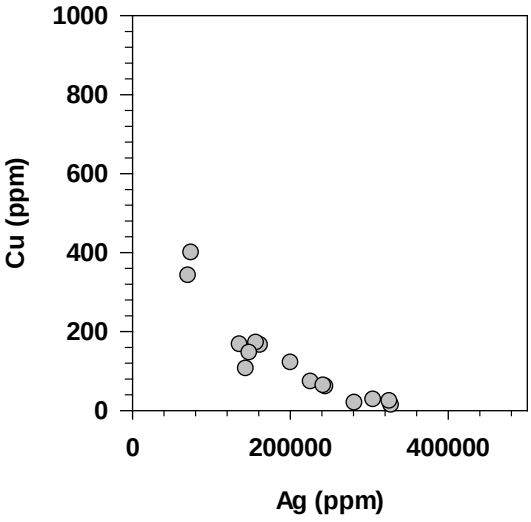
Lower Antler
Cu (ppm)
1000
800
600
400
200
0
0
200000
400000
Ag (ppm)

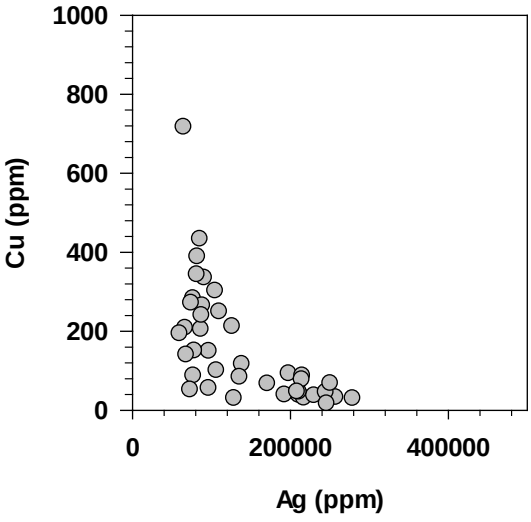
Williams Ck.
Cu (ppm)
1000
800
600
400
200
0
0
200000
400000
Ag (ppm)

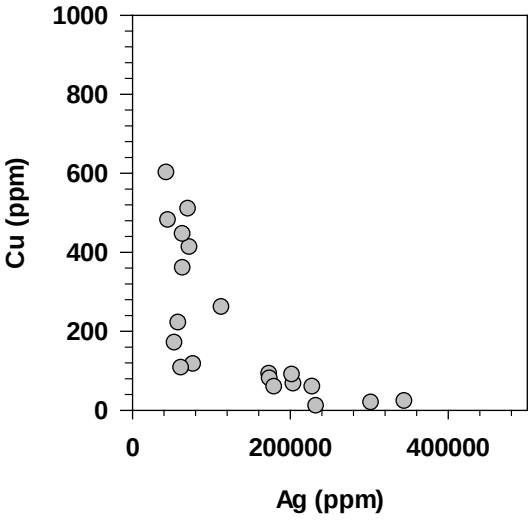
Upper Chishdam
Cu (ppm)
1000
800
600
400
200
0
0
200000
400000
Ag (ppm)

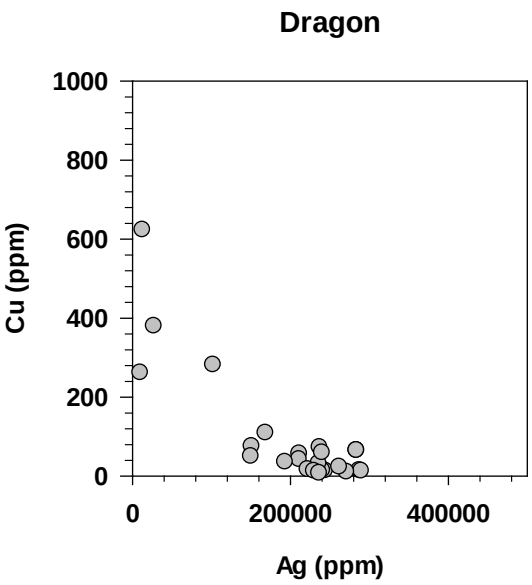
Dragon
Cu (ppm)
1000
800
600
400
200
0
0
200000
400000
Ag (ppm)

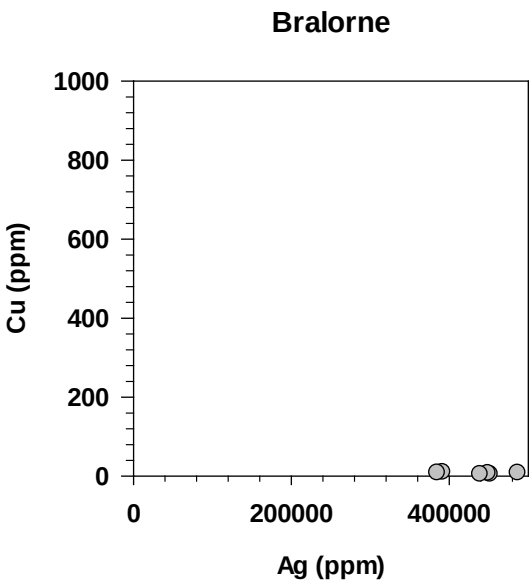
Bralorne
Cu (ppm)
1000
800
600
400
200
0
0
200000
400000
Ag (ppm)

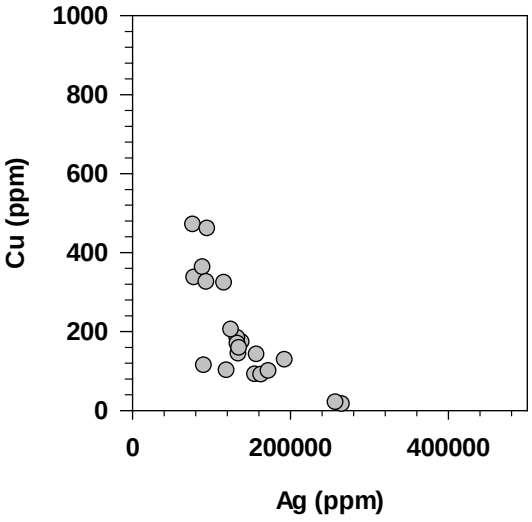
Cunningham Ck.
Cu (ppm)
1000
800
600
400
200
0
0
200000
400000
Ag (ppm)

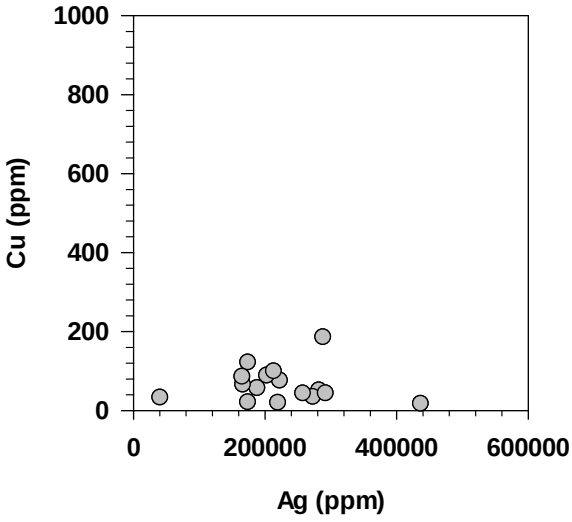
Ruby Ck.
Cu (ppm)
1000
800
600
400
200
0
0
200000
400000
600000
Ag (ppm)

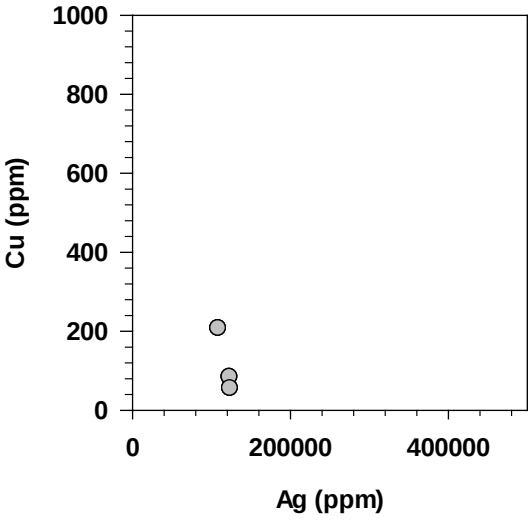
McDame
Cu (ppm)
1000
800
600
400
200
0
0
200000
400000
Ag (ppm)

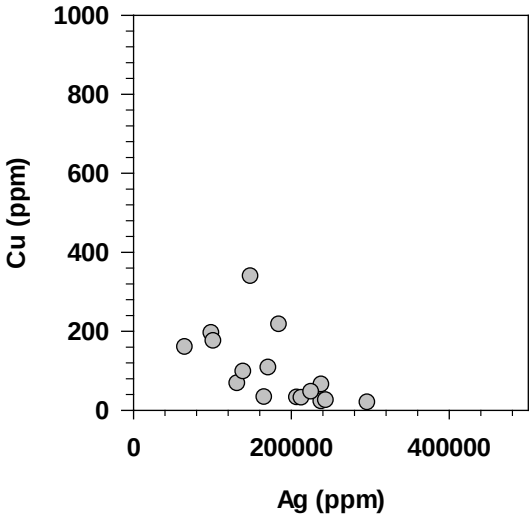
Feather Ck.
Cu (ppm)
1000
800
600
400
200
0
0
200000
400000
Ag (ppm)

Friday Ck.

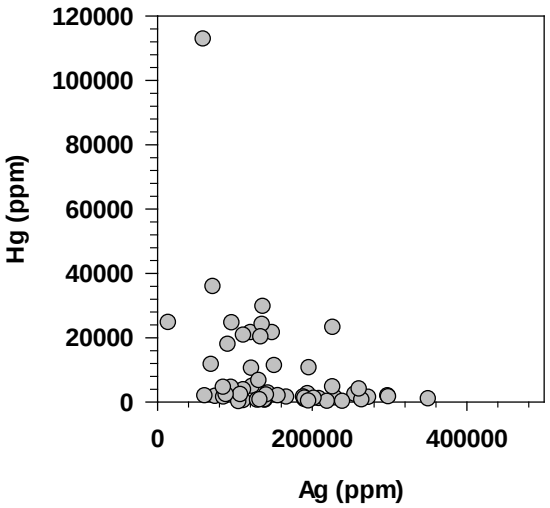

Cherry Ck.

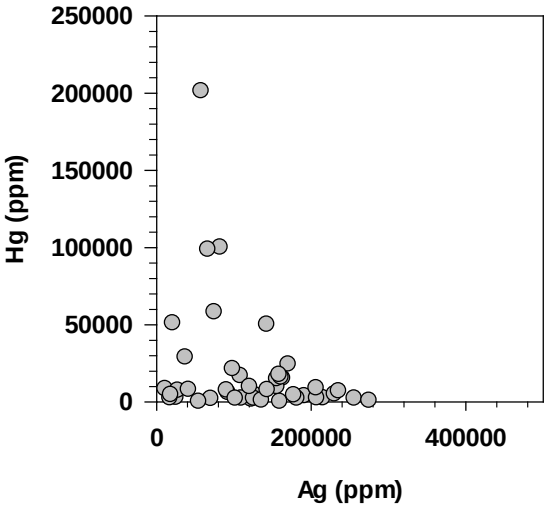

Whipsaw Ck.

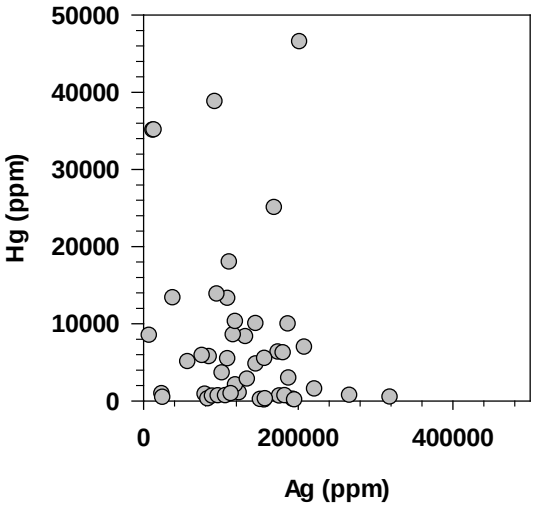

King Richard Ck.

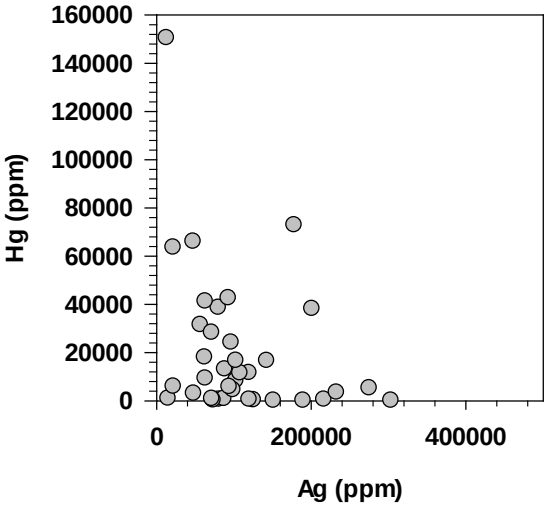

Similkameen

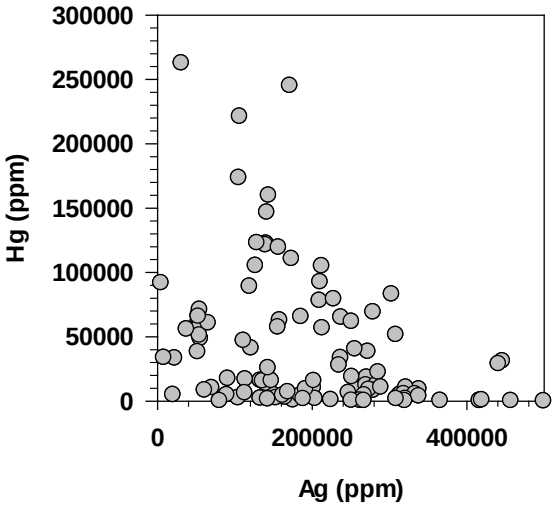

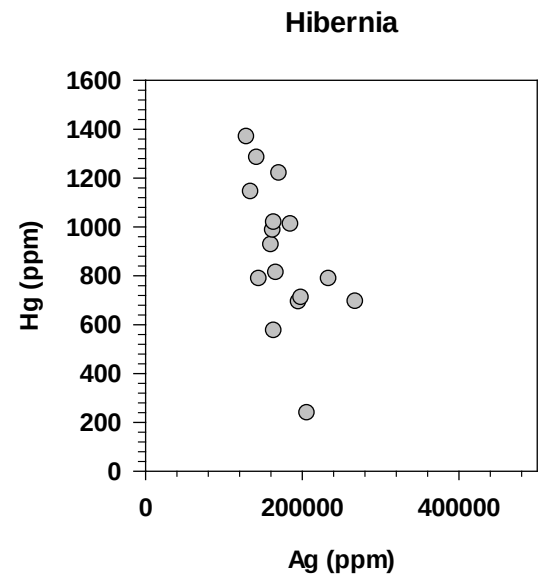
Hibernia
Hg (ppm)
Ag (ppm)
0
200
400
600
800
1000
1200
1400
1600
0
200000
400000

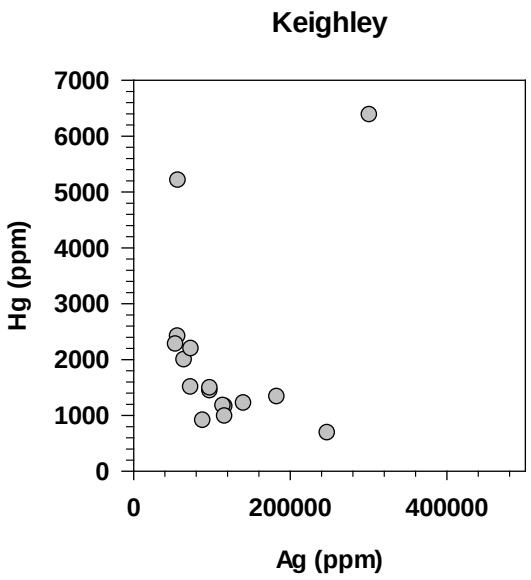
Keighley
Hg (ppm)
Ag (ppm)
0
1000
2000
3000
4000
5000
6000
7000
0
200000
400000

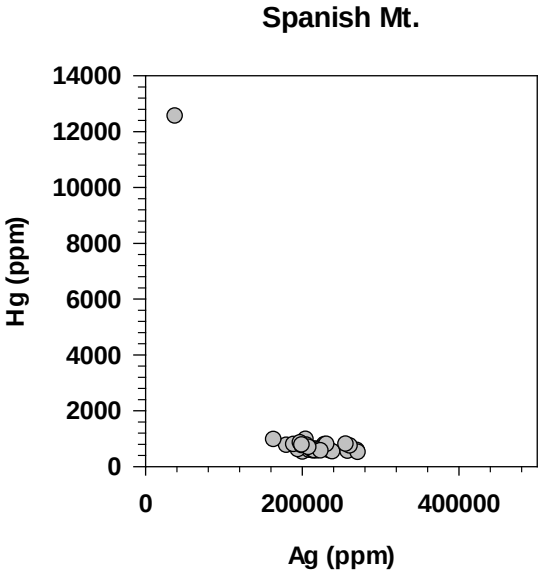
Spanish Mt.
Hg (ppm)
Ag (ppm)
0
2000
4000
6000
8000
10000
12000
14000
0
200000
400000

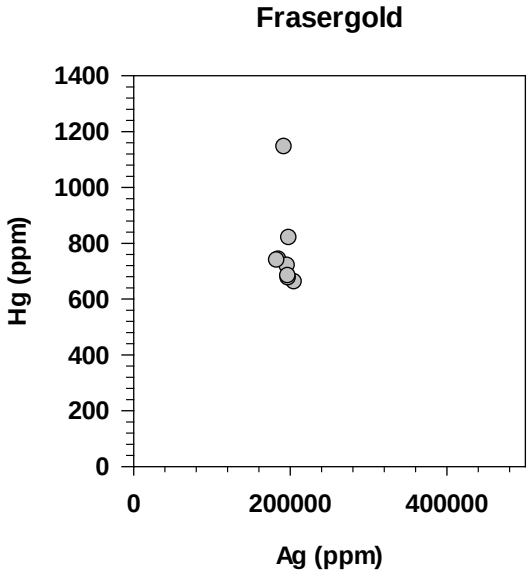
Frasergold
Hg (ppm)
Ag (ppm)
0
200
400
600
800
1000
1200
1400
0
200000
400000

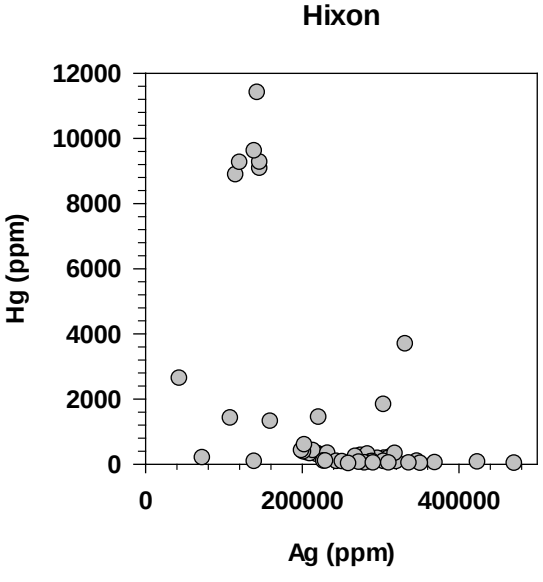
Hixon
Hg (ppm)
Ag (ppm)
0
2000
4000
6000
8000
10000
12000
0
200000
400000

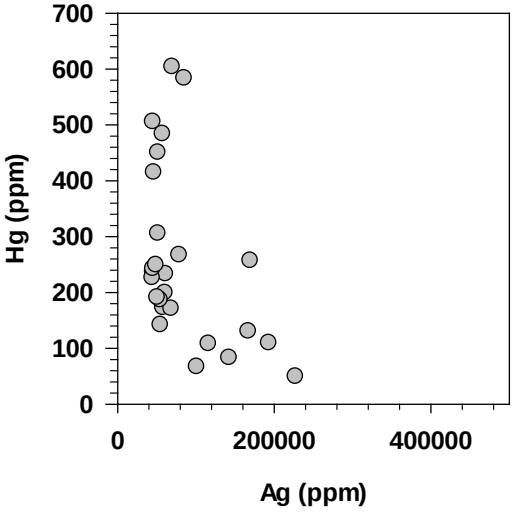
Burns Ck.
Hg (ppm)
Ag (ppm)
0
100
200
300
400
500
600
700
0
200000
400000

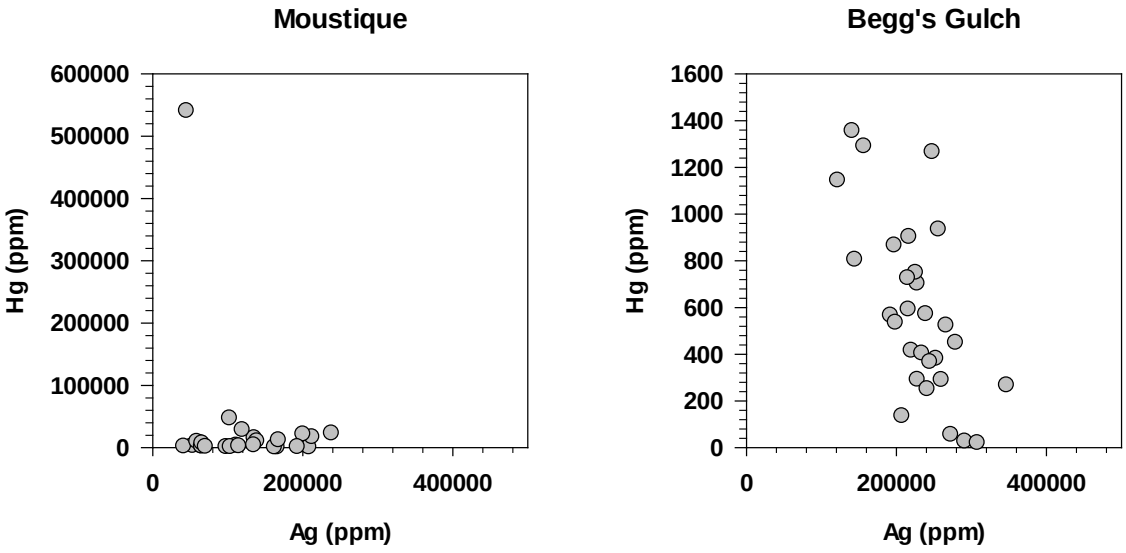
Moustique
Hg (ppm)
600000
500000
400000
300000
200000
100000
0
0
200000
400000
Ag (ppm)

Begg's Gulch
Hg (ppm)
1600
1400
1200
1000
800
600
400
200
0
0
200000
400000
Ag (ppm)

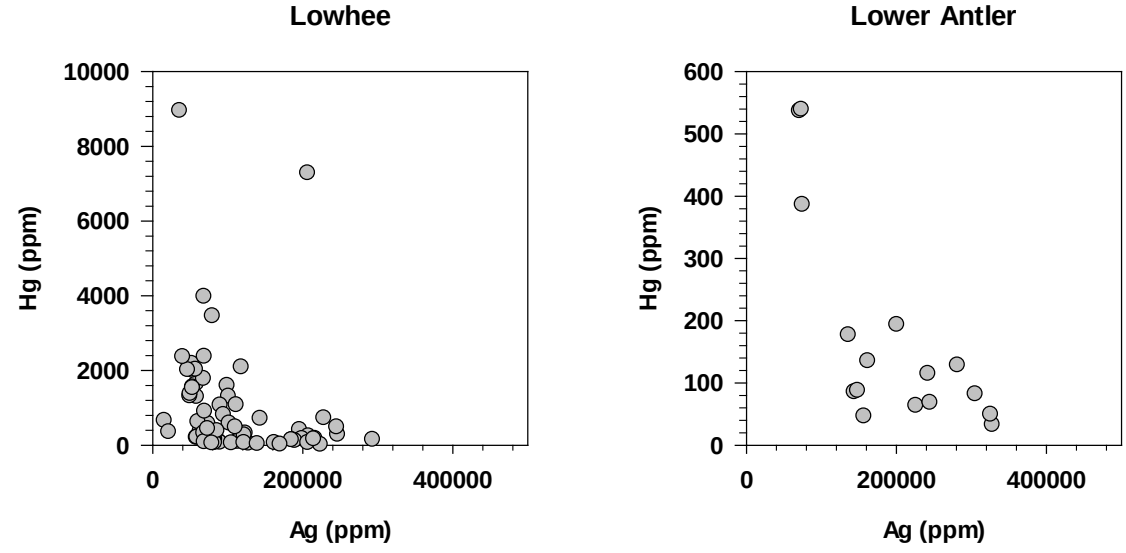
Lowhee
Hg (ppm)
10000
8000
6000
4000
2000
0
0
200000
400000
Ag (ppm)

Lower Antler
Hg (ppm)
600
500
400
300
200
100
0
0
200000
400000
Ag (ppm)

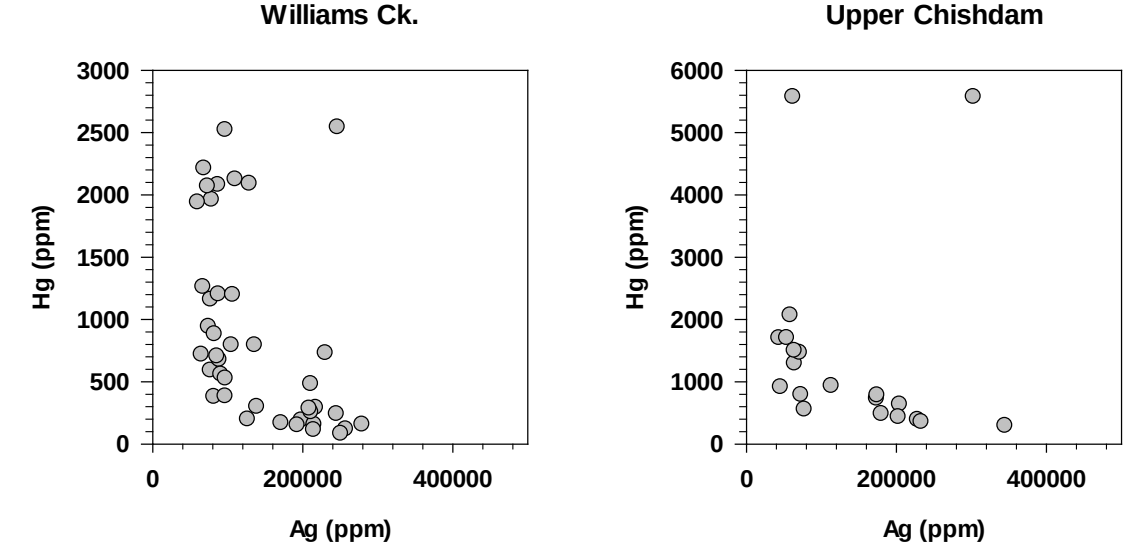
Williams Ck.
Hg (ppm)
3000
2500
2000
1500
1000
500
0
0
200000
400000
Ag (ppm)

Upper Chishdam
Hg (ppm)
6000
5000
4000
3000
2000
1000
0
0
200000
400000
Ag (ppm)

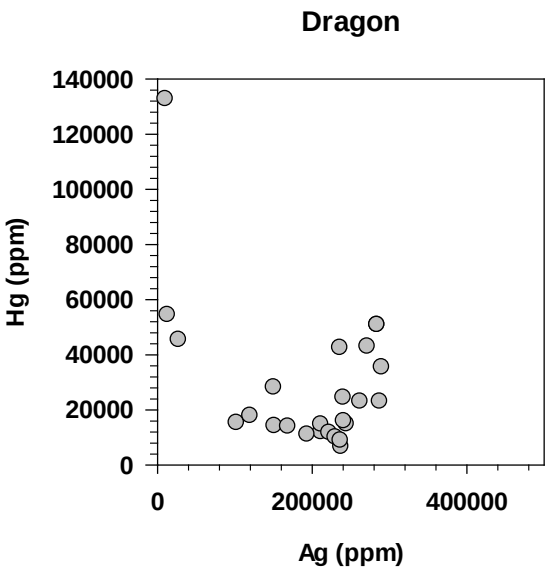
Dragon
140000
120000
100000
80000
60000
40000
20000
0
Hg (ppm)
0
200000
400000
Ag (ppm)

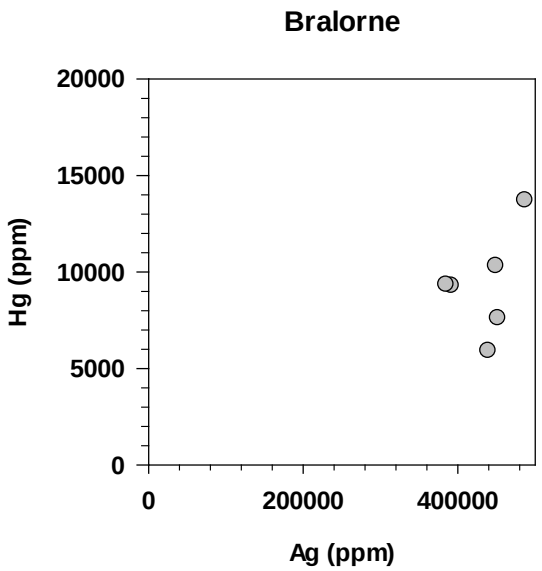
Bralorne
20000
15000
10000
5000
0
Hg (ppm)
0
200000
400000
Ag (ppm)

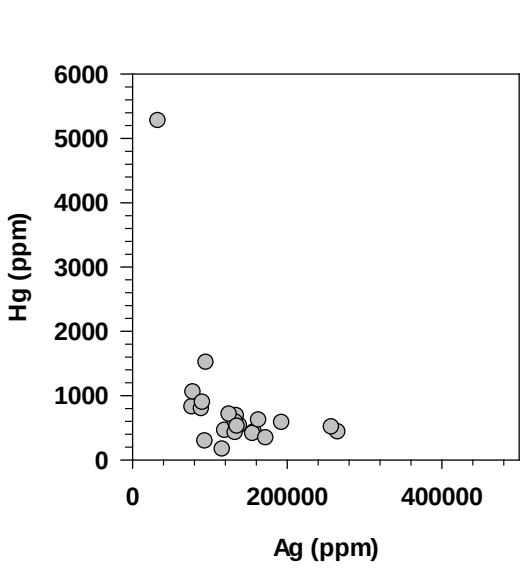
6000
5000
4000
3000
2000
1000
0
Hg (ppm)
0
200000
400000
Ag (ppm)

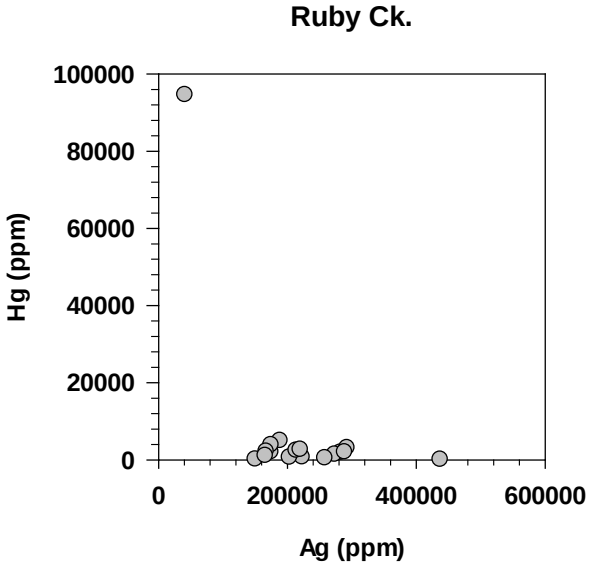
Ruby Ck.
100000
80000
60000
40000
20000
0
Hg (ppm)
0
200000
400000
600000
Ag (ppm)

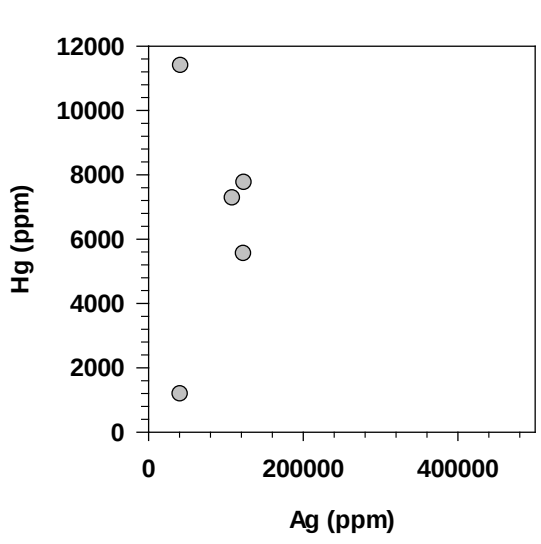
McDame
12000
10000
8000
6000
4000
2000
0
Hg (ppm)
0
200000
400000
Ag (ppm)

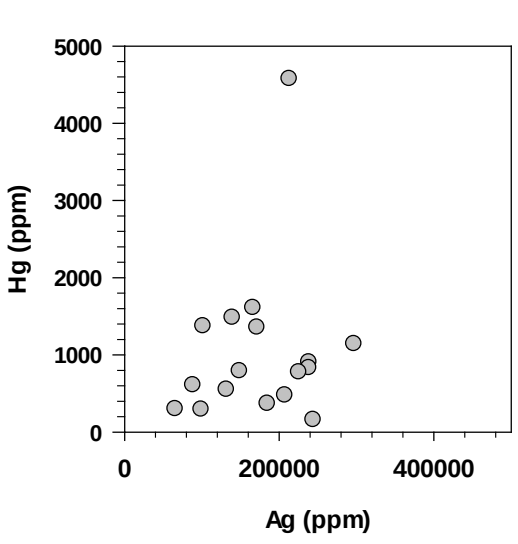
Feather Ck.
5000
4000
3000
2000
1000
0
Hg (ppm)
0
200000
400000
Ag (ppm)